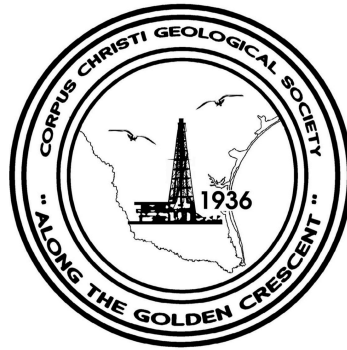


BULLETIN

**Corpus Christi
Geological Society**



and

**Coastal Bend
Geophysical Society**



**March
2016
ISSN 0739 5620**

American Shoreline, Inc.



Specializing in
Oil & Gas Exploration
& Wind Energy

Compliments of

Paul Strunk, Chief Executive Officer
Dennis Taylor, President & Chief Geologist
Jena Nelson, VP Finance & Administration

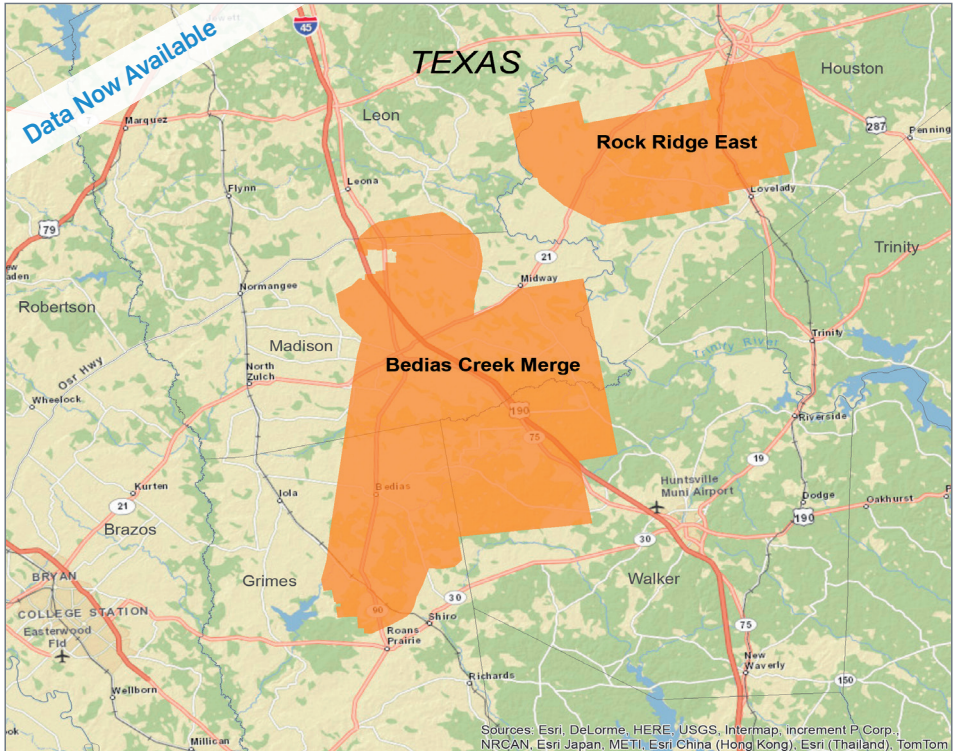
802 N. Carancahua
Frost Bank Plaza, Suite 1250
Corpus Christi, Texas 78401
(361) 888-4496

www.amshore.com



Bedias Creek Merge Madison, Grimes, Walker, and Leon Counties, Texas

YOU'VE ARRIVED



CGG offers the industry's most recent and technologically advanced multi-client data library in the world's key locations. Here is what Bedias Creek has in store:

- 110-fold data acquired using cableless **Sercel UNITE** crews and a dynamite source
- State-of-the-art processing, including 5D Interpolation and Orthorhombic Pre-Stack Time Migration

The best data, the right location, the right time!

Scott Tinley
 +1 832 351 8544
 scott.tinley@cgg.com

Cheryl Oxsheer
 +1 832 351 8463
 cheryl.oxsheer@cgg.com



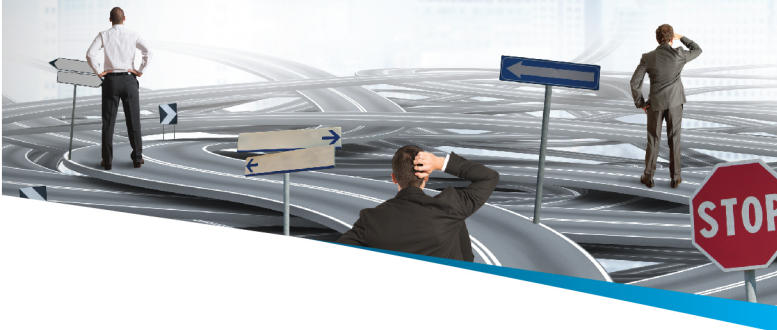
cgg.com/multi-client

TABLE OF CONTENTS

Officers, Committees, and Chairpersons, CCGS, CBGS.....	4 & 5
Calendar of Meetings and Events.....	6 & 7
CCGS President’s Letter.....	9
GCAGS 2016 Explore the Future Sponsorship.....	10,11,12
Gulf Coast Gem & Mineral Show.....	13
Blood Drive.....	14
CBGS President’s Letter.....	15
Luncheon Meeting Announcement.....	18
CCGS Scholarship Application.....	23,24,25
Publications from the BEG Bookstore for GCAGS Materials.....	27-30
A Comparison between methods that discriminate fluid content in unconsolidated sandstone reservoirs—Fred Hilterman.....	32
CCGS papers available for purchase at the Bureau of Economic Geology.....	50
Geo Link Post.....	51
Type Logs of South TexasFields.....	52
Wooden Rigs Iron Men.....	53
Order OIL MEN DVD.....	54
Professional Directory.....	55

Licensing Data?

Don't Let Tape Copy Costs - Drive Your Decision



NEGOTIATE
your tape copies of field data
BEFORE signing contract.

What are your well costs?

\$3 MM, \$5 MM, \$10 MM

100 Square miles of true
CA/CP PSTM re-processing
≈ **\$150,000**

100 Square miles of tape
copy charges
≈ **\$20,000 - \$40,000**

DON'T YOU OWE IT

to **YOURSELF** and
YOUR COMPANY

to have the best image
before drilling?

OUR SERVICES

- Onshore and OBC Controlled Amplitude & Controlled Phase (CA/CP) Processing
- Surface Consistent Processing
- Seamless Multi-Survey Merge
- Gather Conditioning with AVO Attributes
- Inversion and Fluid / Lithology Prediction

SENIOR PROCESSING GEOPHYSICISTS

- Daniela Smoleanu / Partner
- Karen Chevis-McCoy / Partner
- Steven Larson / Partner

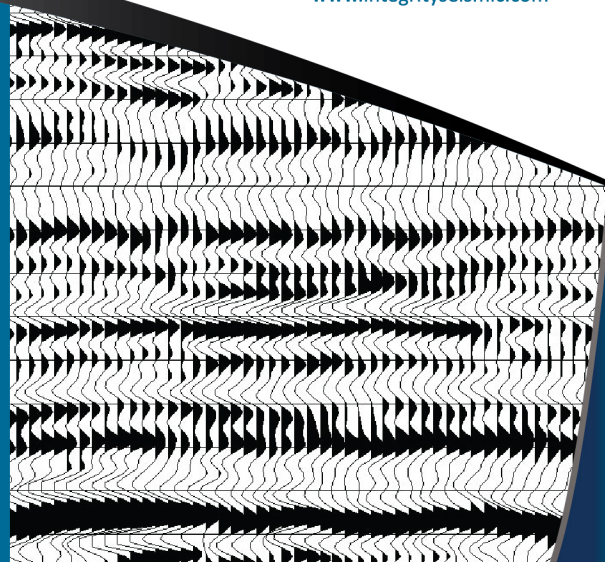


(713)357-4706

www.integrityseismic.com

Zane Swope
President - Partner
(713)357-4706 Ext 7006
(281)635-9162 (Cell)
zswope@integrityseismic.com

James Bloomquist
Business Development Manager
(713)357-4706 Ext 7008
(281)660-9695 (Cell)
Jbloomquist@integrityseismic.com





CORPUS CHRISTI GEOLOGICAL SOCIETY

P.O. BOX 1068 * C.C. TX. 78403

2015-2016

www.ccgeo.org

OFFICERS

President	Mike Lucente	361-883-0923	mikel@impexploration.com
President Elect	Barbara Beynon	361-387-9400	bbeynon77@yahoo.com
Vice President	William Thompson	361-242-3113	William.Thompson@rrc.texas.gov
Secretary	Casey Mibb	361-726-1092	clmibb@yahoo.com
Treasurer	Austin Nye	361-452-1435	austin@nyexp.us
Past President	Leighton Devine	361-510-8872	ldevine@suemaur.com
Councilor I	Rick Paige	361-884-8824	rickp@suemaur.com
Councilor II	Randy Bissell	361-885-0113	randyb@headington.com

AAPG DELEGATE

2006-2016	Dennis Moore	361-886-5144	dennis.moore@bakerhughes.com
-----------	--------------	--------------	--

EDITORS

Bulletin Editor	Marian Wiedmann	361-855-2542	wiedgulf@gmail.com
Bulletin Tech. Editor	Sebastian Wiedmann	361-946-4430	swiedmann.geo@gmail.com
Web Master	Josh Pollard	361-654-3100	support@interconnect.net

GEOLOGICAL SOCIETY COMMITTEES & CHAIRPERSONS

Advertising/ Business Cards	Robert Sterett	361- 739-5618	robert.sterett@gmail.com
Arrangements	Wes Gisler & Will Graham	830-239-4651 361-885-0110	wes@gislerbrotherslogging.com willg@headingtonenergy.com
Bloodmobile	Mike Lucente	361-883-0923	mikel@impexploration.com
Earth Day	Alan Costello	361-888-4792	acostello@royalcctx.com
Continuing Ed.	Stephen Thomas	361-660-8694	stthomas@spnaturalresources.com
Education	J. R. Jones	361-779-0537	jrjones5426@aol.com
Scholarship	Dawn Bissell	361-960-2151	bissells@swbell.net
Fishing Tournament	Leighton Devine	361-882-8400	ldevine@suemaur.com

History	Ray Govett	361-855-0134	ray30@hotmail.com
Membership	Dorothy Jordan	361-885-0110	dorothyj@headington.com
	Randy Bissell	361-885-0113	randyb@headington.com
Type Logs	Frank Cornish	361-883-0923	frank.cornish@gmail.com
University Liaison	Zach Corcoran	361-902-2857	zcorcoran1982@gmail.com



COASTAL BEND GEOPHYSICAL SOCIETY
P.O. BOX 2741 * C.C. TX. 78403
2015-2016

OFFICERS

President	Lonnie Blake	361-883-2831	lonnie_blake@eogresources.com
Vice President	Tom Harrington	361-902-2886	tom_harrington@eogresources.com
Secretary/ Treasurer	Matt Hammer	361-888-4792	mhammer@royalcctx.com

COMMITTEES AND CHAIRPERSONS

Membership	Dorothy Jordan	361-885-0110	dorothyj@headington.com
	Randy Bissell	361-885-0113	randyb@headington.com
Golf Chairman	Fermin Munoz	361 960-1126	fmunoz04@hotmail.com
Scholarship/ Chairman	Ed Egger	361-947-8400	edegger69@gmail.com
Education			

**Visit the geological
Web site at
www.ccgeo.org**

CCGS/CBGS JOINT MEETING SCHEDULE 2015-2016

September 2015							October 2015							November 2015						
S	M	T	W	Th	F	S	S	M	T	W	Th	F	S	S	M	T	W	Th	F	S
		1	2	3	2	5					1	2	3	1	2	3	4	5	6	7
6	7	8	9	10	11	12	4	5	6	7	8	9	10	8	9	10	11	12	13	14
13	14	15	16	17	18	19	11	12	13	14	15	16	17	15	16	17	18	19	20	21
20	21	22	23	24	25	26	18	19	20	21	22	23	24	22	23	24	25	26	27	28
27	28	29	30				25	26	27	28	29	30	31	29	30					

Sept. 10, 2015
5:30p.m.—8:30p.m.
Kickoff BBQ
Hoegemeyer’s Barbeque Barn

Oct. 28—11:30a.m.—1:00p.m.
Speaker: Neil Peake, CCG Geo
Consulting Seismic Reservoir
Characterization.
“Unconventional Reservoirs:
An Integated Workflow
Incorporating Surface Seismic,
Mineralogy, & rock Properties
in the Haynesville Shale.”

Nov. 18—11:30a.m.—1:00p.m.
Speaker: Lorenzo Garza & Joe
Stasulli, Railroad Commission of
Texas. “Horizontal Drilling in Texas:
A Tale That Begins in the Austin
Chalk, but Whose Ending Has Yet
To be Written.”

December 2015							January 2016							February 2016						
S	M	T	W	Th	F	S	S	M	T	W	Th	F	S	S	M	T	W	Th	F	S
		1	2	3	4	5						1	2		1	2	3	4	5	6
6	7	8	9	10	11	12	3	4	5	6	7	8	9	7	8	9	10	11	12	13
13	14	15	16	17	18	19	10	11	12	13	14	15	16	14	15	16	17	18	19	20
20	21	22	23	24	25	26	17	18	19	20	21	22	23	21	22	23	24	25	26	27
27	28	29	30	31			24	25	26	27	28	29	30	28	29					

Dec. 9—11:30a.m.--1:00p.m.
Speaker: Dmitri Bevc, Ph.D.,
Chevron, SEG Distinguished
Lecturer “Full Wave-Form
Inversion: Challenges,
Opportunities and impact”

Jan. 20--11:30a.m.—1:00p.m.
Speaker: Charles Sicking, VP
of R&D/Chief Geophysicist,
Global Geophysical Services,
Inc. “Predicting Frac
Performance and Active
Producing Volumes Using
Microseismic Data”

Feb. 17—11:30a.m.—1:00p.m.
Speaker: Richard Coffin, Ph.D.,
Dept. Chair, Physical & Envir.
Sciences, Texas A&M Univ.—
Corpus Christi. “Integration of
Geochemistry & Geophysics Applied
to Coastal Gas Hydrate
Assessment”

CCGS/CBGS JOINT MEETING SCHEDULE 2015-2016

March 2016							April 2016							May 2016						
S	M	T	W	Th	F	S	S	M	T	W	Th	F	S	S	M	T	W	Th	F	S
		1	2	3	4	5						1	2	1	2	3	4	5	6	7
6	7	8	9	10	11	12	3	4	5	6	7	8	9	8	9	10	11	12	13	14
13	14	15	16	17	18	19	10	11	12	13	14	15	16	15	16	17	18	19	20	21
20	21	22	23	24	25	26	17	18	19	20	21	22	23	22	23	24	25	26	27	28
27	28	29	30	31			24	25	26	27	28	29	30	29	30	31				

March 16-11:30a.m.-1:00p.m.
 Speaker: Thomas Ewing,
 Ph.D., Texas Bureau of
 Economic Geology; Frontera
 Exploration Consultants, Inc.;
 Yegua Energy Associates, LLC
 “Building Texas: Insights from
 the “Texas Through Time
 Project”

April 20-11:30a.m.-1:00p.m.
 Speaker: Lee Billingsley,
 Ph.D., Abraxas Petroleum
 Corp. “Geoscience
 Applications to Economic
 Development of a Relatively
 Shallow, Low Gravity,
 Structurally Complex Eagle
 Ford Oil Development,
 Atascosa County, Texas”

May 18-11:30-1:00p.m.
 Distinguished Speaker: State
 Representative Todd
 Hunter, District 32

Calendar of Meetings and Events Calendar of Area Monthly Meetings

Corpus Christi Geological/Geophysical Society.....	Third Wed.—11:30a.m.
SIPES Corpus Christi Luncheons.....	Last Tuesday—11:30a.m.
South Texas Geological Society Luncheons.....	Second Wed—noon San Antonio
San Antonio Geophysical Society Meetings.....	Fourth Tuesday
Austin Geological Society.....	First Monday
Austin Chapter of SIPES.....	First Thursday
Houston Geological Society Luncheons.....	Last Wednesday
Central Texas Section of Society of Mining Metallurgy & Exp....	2 nd Tues every other month San Antonio

SPONSORS

KNOWLEDGE REVEALED

PURPOSE DRIVEN

- Unrivaled land seismic acquisition capabilities
- Specific solutions for all terrains and environments (land, shallow water/transition zone and OBC)
- Purpose driven crews with proven experience around the world
- Processing and Interpretation services revealing the project knowledge you need
- Full azimuth 3D and 3C coverage in unconventional resource plays
- Multi-Client opportunities in North America, Latin America and Australasia
- Proven experience in:
 - Azimuthal anisotropy resolution and fracture identification
 - Multicomponent processing
 - AVO processing and inversion



INNOVATIVE
GEOPHYSICAL
SOLUTIONS



geokinetics.com



PRESIDENT'S LETTER

URGENT REQUEST TO CCGS & CBGS MEMBERS

This downturn has become quite a problem for us. We have about a dozen members who have volunteered to help with the upcoming convention in September, and that is greatly appreciated. Things are progressing in-so-far as poster sessions, presentations and field trips, but we are desperate for more industry or personal sponsors for the convention.

I urge each and every one of you to put a call or a personal visit with just one company or individual to pledge a sponsorship. This slowdown has caused us to be SHORT OF FUNDS.

We have approximately 300 members. We need your individual help. The dozen volunteer members are overworked and certainly underpaid. Please help your society.

Mike Lucente
CCGS President



2016 GULF COAST ASSOCIATION
OF GEOLOGICAL SOCIETIES
ANNUAL CONVENTION

CORPUS CHRISTI, TEXAS



GCAGS 2016 BOARD

President

Brent Hopkins
Suemaur E&P
361-884-8824, ext 53
bhopkins@suemaur.com

GCAGS2016 Convention

General Chairman

Dawn Bissell
Advent Geoscience Consulting
361-960-2151
bissells@swbell.net

GCAGS2016 Convention

Treasurer

Leighton Devine
Suemaur E&P
361-884-8824, ext 57
ldevine@suemaur.com

GCAGS2016 Convention.

Technical Program

Bob Critchlow,
Virtex Operating
361-882-3046
bcritchlow@virtexoperating.com

GCAGS2016 Convention

Technical Program

Rick Paige
Suemaur E&P
361-884-8824, ext 27
techprogramchair@gcags2016.com

GCAGS2016 Convention

Sponsorships

Lonnie Blake
EOG Resources
361-876-6614
Sponsorships@gcags2016.com

GCAGS2016 Convention

Transactions Editor

Jennifer Smith-Engle
Texas A&M Corpus Christi
361-825-2436
Jennifer.Smith-Engle@gcags2016.com

January 2016

Greetings

The Corpus Christi Geological Society is organizing the Gulf Coast Association of Geological Societies annual convention to be held at the American Bank Center, Corpus Christi, Texas from the 18st to the 20th of September, 2016. The deadline to get your organizations sponsorship in the convention packet is Feb 15th. Sponsorships received after that date will be posted on the website and at the convention venue, but not in the packet.

The GCAGS Convention is a great way to put your organization forward:

- GCAGS has 9000 members, the largest AAPG Section
- 600 -1000 geoscientists and their companies attend the convention
- Professionals from 14 states and 2 countries attended in 2015
- Corpus Christi, the “Sparkling City by the Sea”, a popular GCAGS site
- A very cost effective program to attend/publicize your organization

Proceeds from the annual convention fund every program that the GCAGS does, including: Student and Faculty research grants, the Visiting Professor program, Scholarship Fund Matching program, Student Chapter (AAPG) Leadership Summit travel assistance, Gulf Coast Section of Imperial Barrel Award Competition, Professional Honors and Awards, Teacher of the Year Awards, The GCAGS *Transactions*, and the GCAGS *Journal*.

Sponsoring companies will gain added publicity and acknowledgement throughout the entire Convention. In addition, sponsoring companies will gain longer term advertising exposure through acknowledgement pages at the beginning of the *GCAGS Transactions* publication. The following Sponsorship Levels are available:

Double Diamond - Highest Contributing Sponsor

Diamond	\$25,000
Emerald	\$15,000
Sapphire	\$5,000
Topaz	\$1,000
Patron	\$500

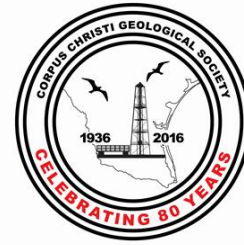
To have your company prominently listed as one of the key sponsors of the upcoming convention please return the attached sponsorship form. If you have any questions, please contact Lonnie Blake at sponsorships@gcags2016.com, or Dawn Bissell at bissells@swbell.net at 361.960-2151 for details.

Lonnie Blake, Sponsorship Chairman
361-876-6614



2016 GULF COAST ASSOCIATION
OF GEOLOGICAL SOCIETIES
ANNUAL CONVENTION

CORPUS CHRISTI, TEXAS



The Gulf Coast Association of
Geological Societies and the Gulf
Coast Section of SEPM

Corporate Sponsorship Opportunities

Corpus Christi, the “Sparkling City by the Sea”
is always a popular GCAGS venue.

What a great way to put your organization forward:

GCAGS – 9000 members, the largest AAPG Section

- 600 - 1000 geoscientists attend
- 900 Professionals representing
450 companies from 14 states and
2 countries attended in 2015

Benefits of sponsorship

- Reinforce your company's name and logo
- Visibility in the exhibit hall
- Stand out from your competitors - give your products and services and edge
- Enhance your standing in the industry
- Earn a profile among young geoscientists - your future workforce

Sponsorship packages - designed to maximize your investment

- Diamond (D) \$25,000+
- Emerald (E) \$15,000+
- Sapphire (S) \$5,000+
- Topaz (T) \$1,000+
- Patron (P) \$500+

Sponsor an event or product - for even more visibility

A sponsorship package can include your name and brand on one of these events,
products, or publications. Choose from among:

- Convention portfolio bag - \$50K exclusive logo/\$25K joint logos
- Icebreaker reception - \$25K exclusive
- All-Convention luncheon - \$25K exclusive
- Presidents' reception - \$25K exclusive
- Field trips & short courses - \$25K exclusive
- Poster sessions - \$10K exclusive
- Judges'/Speakers'/Poster Presenters' breakfast - \$5K exclusive
- Technical session rooms - \$5K per room exclusive for duration of
convention
- Coffee breaks - \$5K exclusive

Package Benefits

(depending on level)

- Complimentary Registrations
(based on sponsorship level:
D-5, E-3, S-2, T-1)
- Logo on banners and signs
posted in exhibit hall and
elsewhere
- Recognition at keynote
speaker address
- Pre- and post-show attendee
mailing lists
- Thank-you recognition in the
convention program book
- Company name and link on
website
- Ads in Transactions volume:
 - D—full-page color
 - E—full-page black & white
 - S—half-page black & white
 - T—quarter-page black & white
 - P—logo(all ads on Transactions CD can
be in color)

GCAGS 2016 will prove to be a great opportunity to build your goodwill and brand.
For more information or to make your sponsorship commitment contact:

Lonnie Blake: Phone 361-876-6614
sponsorships@qcags2016.com
-or-
Dawn Bissell: Phone 361-960-2151
bissells@swbell.net



The Gulf Coast Association of Geological Societies
And the Gulf Coast Section of SEPM

66th Annual GCAGS Convention

September 18-20, 2016

Corpus Christi, Texas

CORPORATE SPONSORSHIP INVOICE

Sponsoring Company _____

Amount _____

Contact Person _____

Email _____

Confirm Here How You Want Your Sponsor Name to Appear: _____

If You Have a Logo You Would Like the GCAGS to Use Please Email It To: gcags2016sponsorship@gmail.com

Mail This Form with Your Check (payable to 'GCAGS 2016') To:

ATTN: GCAGS 2016
Corpus Christi Geological Society
PO Box 1068
Corpus Christi, Texas 78403

Amount _____

Sponsor Package _____



Sponsorship Packages:

- Diamond (D) \$25,000+
- Emerald (E) \$15,000+
- Sapphire (S) \$5,000+
- Topaz (T) \$1,000+
- Patron (P) \$500+

Thank you for your generous support!

Gulf Coast Gem & Mineral Society

54th

Gem, Mineral, Jewelry, & Fossil Show



Sat. March 5th, 2016 10am – 6pm

Sun. March 6th, 2016 10am – 5pm

Displays & Shopping for Everyone

- **free parking**
- **kids wheel**
- **touch table**
- **silent auction**
- **mineral & gem identification**
- **kids 12 and under FREE**
- **and much more**



**Richard M Borchard Regional Fairgrounds,
Building A, 1213 Terry Shamsie Blvd.
Robstown, TX 78380**

www.gcgms.org

BLOOD DRIVE

THE BLOODMOBILE – IN MARCH, 2016
WILL BE AT SOME CONVENIENT LOCATIONS
PLEASE CALL 855-4943 for those locations or see below

*Feeling Lucky this Month? Make someone feel lucky by
donating your Blood!
You'll be glad you did!*



Happy St. Patrick's Day too!

ATTENTION!!!

When you give blood: They have us listed as C.C. Geological Society. Our number with them is 4254 & it would be helpful if you can give them that number also.

**FOR CURRENT SCHEDULES & LOCATIONS OF THE
BLOODMOBILES YOU CAN LOG ON TO:**

www.coastalbendbloodcenter.com

This message approved by Mike Lucente....



CBGS PRESIDENT'S LETTER

News -

News continues to be commodity prices. Looks like the production/consumption gap is narrowing. The first exported LNG from Cheniere Energy's Sabine Pass terminal in southwest Louisiana with the Energy Atlantic LNG tanker is expected during late February/early March 2016. Cheniere's Corpus Christi LNG terminal is expected to begin operations in early 2018.

AND On New Year's Eve, a tanker--the Theo T.--pulled out of Corpus Christi, Texas, with roughly 400,000 barrels of crude supplied by ConocoPhillips from the Eagle Ford Shale.

Business -

CBGS golf tournament being scheduled. Scholarship applicants solicited.

Education/Events -

- GSH

Interpretation Technology Symposium/Exhibition - April 13-14 Norris Conf Center, Houston City Centre

Numerous technical luncheons if you happen to be in Houston. Check following link.

[Geophysical Society of Houston Calendar](#)

CBGS has a revenue sharing agreement with GSH. Please mention CBGS if you register for any GSH events.

- SEG

SEG Convention, 16-21 October, Dallas

SEG has 450+ eLearning courses online from \$0.99 to \$150.00(most expensive I saw)

<http://www.seg.org/professional-development/seg-on-demand>

- AAPG

AAPG Convention, 19-22 June, Calgary

- HGS

Mudrocks Conference, 8-9 March, Woodlands

- NAPE

August 10-11, Houston

- OTC

May 2-5, Houston

Thought for the month

Don't be afraid to give your best to what seemingly are small jobs. Every time you conquer one it makes you that much stronger. If you do the little jobs well, the big ones

will tend to take care of themselves. ~Dale Carnegie

Monthly O&G Statistics

Texas Oil and Gas Info	Current Month	Last Month	Difference	
Texas Production	MMBO/BCF	MMBO/BCF	MMBO/BCF	
Oil	78.9	70.9	8	Nov
Condensate	9.8	11.2	-1.4	
Gas	596	666	-70	Nov
	Current Month	Yr to date - 2016	Yr to date - 2015	
Texas Drilling Permits	510	510	1,102	Jan
Oil wells	425	425	971	
Oil and Gas	282	282	697	
Gas wells	41	41	90	
Other	0	0	0	
Total Completions	965	18,510	27,595	Jan
Oil Completions	951	951	1,450	
Gas Completions	197	197	344	
New Field Discoveries	0	0	4	
Other	6	6	30	

Thought for the month:

A vision without a task is but a dream, a task without a vision is drudgery, a vision with a task is the hope of the world
 - Inscription on a wall in Sussex England, circa 1730

Lonnie Blake
 President CBGS

SPONSORS

Performance You Can Count On

An acknowledged leader in today's exploration and production industry, EOG Resources looks ahead.

Annually, EOG is one of the most active drillers in the United States. We grow through the drill bit, rather than seeking major acquisitions or mergers to bolster our reserves and production. This unrelenting focus on organic production growth has proven successful because we have identified significant North American resource plays for tomorrow. Our creative, hardworking explorationists and those who support them utilize the latest technology available in the marketplace, adapting and modifying it to meet the challenges EOG faces. With a focus on returns, EOG continues to produce peer-leading financial and operational results.

In 2013, EOG became the largest onshore oil producer in the Lower 48, and we're still growing.

EOG Resources, Inc.

539 N. Carancahua
Suite 900
Corpus Christi, TX 78401-0908
361-883-9231
www.eogresources.com



EXPLORING SINCE 1968



802 N. Carancahua St
Suite 1000
Corpus Christi, TX 78401-0015
Phone: (361) 884-8824
Fax: (361) 884-9623



**CORPUS CHRISTI GEOLOGICAL SOCIETY
COASTAL BEND GEOPHYSICAL SOCIETY**



LUNCHEON MEETING ANNOUNCEMENT

WEDNESDAY, MARCH 16TH, 2016

- Location:** Congressman Solomon P. Ortiz International Center, 402 Harbor Drive, Corpus Christi, TX 78401 <http://ortizcenter.com>
- Bar Sponsor:** To be announced (*sponsors needed!*)
- Student Sponsor:** Core Laboratories and Global Geophysical Services
- Time:** 11:30 am Bar, Lunch follows at 11:45 am, Speaker at 12:00 pm
- Cost:** \$25.00 (additional \$10.00 surcharge without reservation; No-shows may be billed and non-RSVP attendees cannot be guaranteed a lunch); *FREE* for students with reservation (discounted by our generous sponsors)!
- Reservations:** Please RSVP by 4PM on the FRIDAY before the meeting!
E-Mail: wes@gislerbrotherslogging.com

Please note that luncheon RSVPs are a commitment to the Ortiz Center and must be paid even if you can't attend the luncheon.



<http://www.corelab.com>



<http://www.globalgeophysical.com>

Please thank our generous sponsors!!!

**SPONSORSHIPS FOR THE TUESDAY PINT NIGHT SOCIAL GATHERING AND
WEDNESDAY LUNCHEON MEETING BARS ARE OPEN!!!**

Please consider becoming a CCGS/CBGS sponsor!!!

Building Texas: Insights from the “Texas Through Time” Project

Presented by: Thomas Ewing, Ph.D. – Texas Bureau of Economic Geology, University of Texas - Austin; Frontera Exploration Consultants, Inc.; Yegua Energy Associates, LLC

Summary

In June, 2013, I began work at the Texas Bureau of Economic Geology (BEG) to put together a summary volume on the geology of Texas as geologists currently understand it, to be designed for general audiences. At present, the draft is completed and we are in review and editing/compositing stage; anticipated printing date is February, 2016. The book is fully illustrated in color, and around 360 pages long. It includes a comprehensive series of time-stratigraphic charts and an atlas of paleogeography and other features.

The book begins with a summary of landscapes and regions of the state. Two short chapters focus on general geologic principles and the layering of the earth beneath Texas, and the plate tectonic position of Texas through geologic time. Four subsequent chapters tell the story of Texas history from Proterozoic through Cenozoic, then into the Holocene. Finally, two chapters survey Texas resources and hazards.

To write such a summary involved summarizing and synthesizing hundreds of geological reports and articles. That has led to some interesting new insights, a few of which follow:

- Latest Precambrian-Middle Cambrian rifting includes activity on the Devils River trend at least as far as Van Horn. Interestingly, Cambrian and Ellenburger isopachs don't show subsidence into that area, but instead towards San Antonio.
- One terrane that used to form part of Texas (south of the former Marathon Basin) was detached in the Cambrian and later sheared off to form “Cuyania” in South America. It's possible that Sabinia (the Sabine Block) is also a part of North America and not exotic - but we need crazy deep drilling to be sure!
- Ouachita-Marathon deformation is a 'soft docking' not a high-impact continental collision. It doesn't seem to explain the Late Paleozoic uplifts and basins (ARM), which are more consistent with SW-NE compression and related strike-slip. Compressions from the SW or the ENE (Appalachian collision) are the more likely cause of deformation.
- Permian subsidence overlaps the ARM structuring in time and space, and continues to the end of the Paleozoic. Absence of detrital wedges from Marathon is remarkable, indicating that Permian subsidence continued south of the present-day Marathons.
- Gulf of Mexico extension had two phases. The first extended the region in a SE direction at upper and lower crustal levels. This extension formed a broad, hot and dry basin lying over a thousand feet below sea level, which was then filled by salt as seawater dribbled in. Afterwards, the second phase produced new oceanic crust, which rotated Yucatan over 40° counterclockwise.

- We can look at larger deltas and make intelligent guesses at the rivers that fed them and the highlands that formed sediment. Major streams include a 'Lone Oak River' which drained the Hueco Arch and others areas in the Jurassic and Early Cretaceous; a 'Cox River' draining southwest in the Albian; and a 'Bigfoot River' reaching from Big Bend to central Texas in the late Cretaceous.

The project also includes a website, which forms part of the overall BEG website. It will include statewide information; some material from the book; and a series of 70-plus Great Places to View Texas Geology. These are miniature field trip guides to highlight publicly accessible places to be wowed by Texas rocks and landscapes. Each site includes a nontechnical discussion of what you see, and why it's important; a gallery of photographs; and a few references and websites for more information.

Southeast Texas sites included in the Great Places include: Stone City and Somerville (Eocene), the Rayburn Dam area (Catahoula), LaGrange (Oakville), Brazos Bend (Brazos bottomland), the Liberty/Anahuac (Trinity River and delta), and the Sabine Pass, Bolivar Peninsula and Galveston-Freeport areas in the coastal zone.

In South Texas, these sites include: Goliad-La Bahia (Goliad escarpment), the Aransas Refuge (Ingleside), Padre Island, Roma-Rio Grande City, Sal del Rey, Baffin Bay and the Rio Grande Delta. Northward into Central Texas, familiar sites such as Enchanted Rock and the Inks Lake area are joined by Natural Bridge Caverns, the Uvalde area and the roadcuts out toward Langtry.

About our Presenter:



Dr. Thomas Ewing is a geoscientist with over 33 years of experience in hydrocarbon exploration and research. He is a Registered Professional Geoscientist in the State of Texas (#1320) and an AAPG/DPA Certified Petroleum Geologist (#4538), and holds certification #1610 from SIPES.

He received a B.A. in Geology from the Colorado College (1975), an M.S. in Geochemistry from New Mexico Institute of Mining and Technology (1977), and a Ph.D. in Geological Sciences from the University of British Columbia (1981).

Dr. Ewing was a research geologist for four years at the Texas Bureau of Economic Geology in Austin, working on Gulf Coast geopressured reservoirs, serving as a co-author of the "Atlas of Texas Oil Reservoirs", and compiling the Tectonic Map of Texas. Since 1985 he has been co-owner of Frontera Exploration Consultants, Inc., a San Antonio-based geoscience consulting company; he has consulted to numerous clients in South Texas, New Mexico and elsewhere. He worked with Venus Oil and Venus Exploration from 1985 to 2005 as staff consultant and Senior Explorationist, playing a main role in its successful exploration in the

Yegua Trend of the Gulf Coast Basin, the Cotton Valley trend of Texas and Louisiana, and in West Texas and Kansas. He is now a partner in Yegua Energy Associates, LLC, which is continuing hydrocarbon exploration in these trends.

In 2013, Dr. Ewing received a half-time appointment with the Texas Bureau of Economic Geology as project director to develop "Texas Through Time", an illustrated book and website on the geologic history and earth resources of Texas for a general audience.

Dr. Ewing is a member of many regional and national professional societies. He has served as Treasurer, Vice-President and President (2007-08) of the AAPG Division of Professional Affairs, and has received Life Membership in the DPA (2014). He is an AAPG Delegate from the South Texas Geological Society, and served as Vice-Chairman of the AAPG House of Delegates in 1992-93. He is also served as President of the Energy Minerals Division of the AAPG (1999-2000), and received Honorary Membership in that Division in 2009. Most recently, he completed service as Vice-President for Sections of AAPG (2012-14). He served as President of the South Texas Geological Society in 1990-1991, and as General Chairman of the 1996 GCAGS Convention in San Antonio. He received Honorary Membership in the South Texas Geological Society in 2009, Honorary Membership in the GCAGS in 2010, and BEG Alumnus of the Year in 2011.

Tom has spoken extensively at local, regional, and national geological meetings and published over 75 papers and abstracts. Among other awards, he has twice received the Gulf Coast Section AAPG Levorsen Award (1982 and 1999), and has received the AAPG Distinguished Service Award. He has written articles on Gulf Coast geology and hydrocarbons, the geology and tectonics of Texas, and history and urban geology of the San Antonio area. He wrote the popular guidebook "Landscapes, Water and Man: Geology and Man in the San Antonio Area" published by the South Texas Geological Society in 2008.

In his spare time, he leads field trips in South Texas, and directs a 60-voice German men's chorus, the San Antonio Liederkrantz. Tom will be leading a two-day field trip for the September Gulf Coast Association of Geological Society's Annual Convention studying the geology of two sites in South Texas, the Holocene Rio Grande Delta and the Great Sand Sheet.

sponsors



Winn Exploration Co., Inc.

Actively Seeking High Quality
Drilling Prospects

Contacts:

Mike Layman (Geophysicist)	361-844-6922
Tom Winn (Geologist)	361-844-6992
Southern Winn (Geologist)	361-844-6998

800 North Shoreline Blvd.
19th Floor, North Tower
Corpus Christi, Texas 78401

Office: 361-844-6900 Fax: 361-844-6901

WEL-LAB

HYDROCARBON LOGGING SERVICE



Operating in South Texas and Gulf Coast since 1961

Contact: Mike Bullard

P.O. Box 1011

Kingsville, Texas 78364

361-221-9717

Email: md_bullard@sbcglobal.net

A Great Place For Business

In the heart of the Business District
Broadway at Leopard

- Onsite Management
- Conference Room
- Deli & Vending Room
- Security Card Access
- High Speed Elevators
- View of Corpus Christi Bay

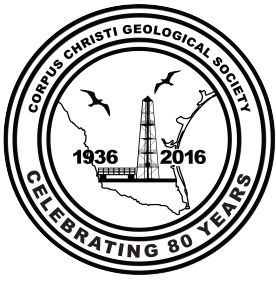
COMMITTED TO EXCELLENCE
Yesterday • Today • Tomorrow

The
600
BUILDING

Contact
Ellen Blasingame
698-6000

ecblasingame@netscape.net





Corpus Christi Geological Society Scholarship Application Guidelines 2016 Summer Field Camp

1. Applicant must be currently attending a college in the local area AND planning to attend Field Camp for the summer of 2016.
2. Applicant must have a 2.5 GPA overall AND a 3.0 GPA in Geology courses.
3. Applicant must be recommended by your faculty for this scholarship.
 - a. See Faculty Recommendation Form *NEW!*
4. Complete the Scholarship Application.
5. Write a short essay explaining your geologic career goals.
6. Provide a school transcript, make sure it has your name on it. A web printout is acceptable.
7. **Applications must be postmarked by: March 31, 2016**
Mail completed application to: Dawn Bissell, CCGS Scholarship Committee Chairman, 253 Circle Drive, Corpus Christi, TX 78411

Email bissells@swbell.net once you've mailed your application. If I do not receive an email, I won't be able to notify you if you've been selected. ***Award notifications will be sent via email!!!***

Please read requirements carefully and submit only complete applications. Applicants who have received a CCGS scholarship in the past are eligible to apply again.

Scholarships will be awarded based on merit and need.

Award recipients will be recognized at the monthly **luncheon April 20, 2016** and are encouraged to attend.

Board Members:

Dawn Bissell - Chairman
Brent Hopkins - Treasurer
Mike Lucente - CCGS President
B.J. Thompson - Member

JR Jones - Vice-Chairman
Beth Priday - Secretary
Bob Critchlow - Member



Corpus Christi Geological Society
Faculty Recommendation for
2016 Summer Field Camp Scholarship
(Must be postmarked by March 31, 2016)

Student's Last Name: _____ First Name: _____

University Currently Attending: _____

University Hosting Field Camp: _____

Has the student Applied to Field Camp for the Summer of 2016? Yes No

Has the student been Accepted? Yes No

Do you recommend this student for this scholarship? Yes No

Comments:

Faculty Signature

Date

University

Mail/Email to Dawn Bissell, CCGS Scholarship Committee Chairman
253 Circle Drive, Corpus Christi, TX 78411 **by March 31, 2016.**
Email bissells@swbell.net



Corpus Christi Geological Society
Scholarship Application Form
2016 Summer Field Camp
(Must be postmarked by March 31, 2016)

Last Name: _____ First Name: _____

Mailing address: _____
(where award may be mailed if you are unable to attend the award presentation)

City: _____ State: _____ Zip Code: _____

Active Email:

Award notifications will be sent via email!!! Email bissells@swbell.net once you've submitted your application.

Daytime Phone: _____ Alternate Phone: _____

University Currently Attending: _____

Department: _____ Major: _____

University Hosting Field Camp: _____

Have you Applied? Yes No; Have you been Accepted? Yes No

Scholarship is for class level (circle one):

Freshman Sophomore Junior Senior Graduate Student

Total Hours Completed: _____ Overall GPA (Minimum 2.5): _____

Total Hours - Geology: _____ Geology GPA (Minimum 3.0) _____


Prior recipient of CCGS Scholarship? Yes No

Applicant Signature

Date

Mail application, along with essay, faculty recommendation form, and transcript to:
Dawn Bissell, CCGS Scholarship Committee Chairman
253 Circle Drive, Corpus Christi, TX 78411 **Must be postmarked by March 31, 2016.**
Email bissells@swbell.net once you've mailed your application. Award notifications will be made via email!!!

SPONSORS



Nueces Energy, Inc.
P.O. Box 252
Corpus Christi, Texas 78403
Office: (361) 884-0435
Fax: (361)-654-1436
www.nuecesland.com

Nueces Energy, Inc. is a complete land services company in the business of providing professional landmen and project management to various energy related jobs primarily in the oil and gas industry.

With over 30 years of industry experience, we specialize in determining surface and subsurface ownership and negotiating and acquiring contracts, rights of way agreements, and easements to provide our clients with the legal right to explore and develop oil and gas resources. We provide a full service land company capable of managing any project no matter how large or small.



THUNDER EXPLORATION, INC.
Celebrating 30+ years of prospect generation and exploration in the following South Texas plays and trends.

Frio	San Miguel	Edwards
Jackson	Austin Chalk	Pearsall
Yegua	Eagle Ford	Sligo
Wilcox	Buda	Cotton Valley
Olmos	Georgetown	Smackover

Thunder is currently seeking non-operated working interest participation in projects and prospects.

Contact **Walter S. Light Jr.**
President/Geologist
713.823.8288
EMAIL: wthunderx@aol.com

Headington Oil Company is now...



HEADINGTON
ENERGY PARTNERS, LLC

Proudly operating in South Texas.

For more information contact:
Randy Bissell, randyb@headingtonenergy.com or call 361-885-0113



Offices in Corpus Christi, Sarita, and McKinney, Texas - Exploring and Developing properties
In South Texas, Permian Basin, East Texas & Oklahoma

Gulf Coast Association of Geological Societies (GCAGS) Titles List

January 2016

<http://begstore.beg.utexas.edu/store/>

GCAGS Bibliography of Gulf Coast Geology

Volumes 1 and 2 cover the literature from pre-1900 to 1968. Volume 1 is the bibliography; Volume 2 is the subject index. (1970).

GCAGS 301B \$5.00

Volume 3 covers the literature for 1969–1974. (1976).

GCAGS 303B \$4.00

Volume 4 covers the literature for 1975–1979. (1982)

GCAGS 304B \$4.00

Volume 5 covers the literature for 1980–1984. (1986).

GCAGS 305B \$5.00

Volume 6 covers the literature for 1985–1989. (1990).

GCAGS 306B \$5.00

Volume 7 covers the literature for 1990–1995, includes index. (1998).

GCAGS 307B \$30.00

GCAGS Journals

Established in 2012, the GCAGS Journal is an annual, mainstream, academic journal comprising peer-reviewed articles on geoscientific topics related to the Gulf of Mexico basin. For more information, please see <http://www.gcags.org/Journal/GCAGS.Journal.html>.

Volume 1, 2012. T. F. Hentz, ed.; J. J. Willis, managing ed. Hardcover, full color, 13 articles, 185 p. ISBN 978-0-0883883-1-4.

GCAGS J01 \$25.00

Volume 2, 2013. T. F. Hentz, ed.; J. J. Willis, managing ed. Hardcover, full

color, 7 articles, 84 p. ISBN 978-0-9883883-2-1.

GCAGS J02 \$25.00

GCAGS Journal, Volume 3 (2014). A Publication of the Gulf Coast Association of Geological Societies. T. F. Hentz, ed.; J. J. Willis, managing ed. Howard Creasey, T. E. Ewing, A. M. Goodliffe, B. J. Katz, R. P. Major, M. J. Nault, and J-P Nicot, associate eds. Hardbound, full color, 10 articles, 134 p., 2014.

GCAGS J03 \$25.00

GCAGS Journal, Volume 4 (2015): A Publication of the Gulf Coast Association of Geological Societies. Hardbound, full color, 9 articles, 2015.

GCAGS J04 \$25.00

GCAGS Maps

Faults of South and Central Texas, Map compiled by D. R. Tucker (1967).

GCAGS 402M \$2.00

Bathymetry of the Gulf of Mexico, Map [by] Elazar Uchupi (1967).

GCAGS 403M \$2.00

GCAGS Publications Indexes

Volume I. Covers *Transactions* Volumes 1–15. Compiled by D. E. Masten and E. J. Prochasta. 84 p., 1966.

GCAGS 101 \$2.50

Volume II. Covers *Transactions* Volumes 16–Volume 31. Compiled by Jules Braunstein, 151 p., 1983.

GCAGS 102 \$2.50

Volume III. Covers *Transactions* Volumes 32–Volume 45 for the years 1982–1995. Compiled by the staff of Datapages, Inc., Tulsa, OK, and QSEP Publishing, Inc., Marlow, NH. 315 p., 1997.

GCAGS 103 \$20.00

GCAGS Readings in Gulf Coast Geology

Volume 2. Petroleum Geology of the Cenozoic of the Central Gulf Coast, with Special Emphasis on the Miocene. Compiled by R. W. Stephens. 10 papers from *GCAGS Transactions*. (1981).
GCAGS 202R \$15.00

Volume 3. Biostratigraphy and Paleoecology of Gulf Coast Cenozoic Foraminifera. Compiled by S. P. Ellison, Jr. 14 papers from *GCAGS Transactions*. (1982).
GCAGS 203R \$10.00

Volume 5. Holocene Sediments of the Gulf of Mexico. Compiled by E. C. Roy, Jr. 15 papers from *GCAGS Transactions*. (1984).
GCAGS 205R \$12.00

Volume 6. The Stratigraphic Factor in Hydrocarbon Reservoirs of the Gulf Coast. Compiled by L. H. Meltzer. 21 papers from *GCAGS Transactions*. (1985).
GCAGS 206R \$10.00

Volume 7. Production and Reservoir Geology of Selected Gulf Coast Oil and Gas Fields. Compiled by J. A. Hartman. 16 papers from *GCAGS Transactions*. (1985).
GCAGS 207R \$10.00

Volume 8. Applications of Sequence Stratigraphy in the Gulf of Mexico Basin. Compiled by B. R. Weise. *GCAGS Readings in Gulf Coast Geology*, CD. (2000).
GCAGS 208R \$30.00

Volume 9. Applications of 3D Seismic Technology in the Gulf of Mexico Basin. Compiled by D. F. Balin. *GCAGS Readings in Gulf Coast Geology*, CD. (2000).
GCAGS 209R \$30.00

GCAGS Special Publications

Field Trip Guide. Guide to 4 field trips for the 36th Annual GCAGS Convention, Baton Rouge, Louisiana. 46 p., 1986.
GCAGS 501SV \$5.00

Montgomery Landing Site, Marine Eocene (Jackson) of Central Louisiana. Proceedings of a Symposium, 36th Annual GCAGS Convention, Baton Rouge, Louisiana. J. A. Schiebout and William van den Bold, eds. 238 p., 1986.
GCAGS 502SV \$5.00

Paleogene Stratigraphy and Biostratigraphy of Southern Alabama, by E. A. Mancini and B. H. Tew. Field Trip Guidebook for the GCAGS/GCS-SEPM 38th Annual Convention, New Orleans, Louisiana. 63 p., 1988.
GCAGS 503SV \$8.00

Geology of the Sierra Catorce Uplift, Kay Greier and Joseph Kowalski, eds. Field Trip Guidebook for the 39th Annual GCAGS Convention, Corpus Christi, Texas, 82 p., 1989.
GCAGS 504SV \$10.00

Structural Framework of the northern Gulf of Mexico. A Special Publication of the Gulf Coast Association of Geological Societies. J. O. Jones and R. I. Freed, eds. Various paginated, 1996. Includes oversized map in pocket.
GCAGS 507SV \$20.00

Gulf Coast Association of Geological Societies (GCAGS) Transactions

A DVD version is available for Volumes 1–63 as a set and for Volumes 50–65 as separate items.

Volume 1 (1951) New Orleans.
GCAGS 001 \$15.00

Volume 2 (1952) Corpus Christi.
GCAGS 002 \$15.00

Volume 3 (1953) Shreveport.
GCAGS 003 \$20.00

Volume 4 (1954) Houston.
GCAGS 004 \$10.00

Volume 5 (1955) Biloxi.
GCAGS 005 \$15.00

Volume 6 (1956) San Antonio.
GCAGS 006 \$20.00

Volume 7 (1957) New Orleans.
GCAGS 007 \$20.00

Volume 8 (1958) Corpus Christi.
GCAGS 008 \$20.00

Volume 9 (1959) Houston.
GCAGS 009 \$20.00

Volume 10 (1960) Biloxi.
GCAGS 010 \$15.00

Volume 11 (1961) San Antonio.
GCAGS 011 \$20.00

Volume 12 (1962) New Orleans.
GCAGS 012 \$15.00

Volume 13 (1963) Shreveport.
GCAGS 013 \$10.00

Volume 14 (1964) Corpus Christi.
GCAGS 014 \$10.00

Volume 15 (1965) Houston.
GCAGS 015 \$15.00

Volume 17 (1967) San Antonio.
GCAGS 017 \$10.00

Volume 18 (1968) Jackson.
GCAGS 018 \$10.00

Volume 19 (1969) Miami.
GCAGS 019 \$10.00

Volume 20 (1970) Shreveport.
GCAGS 020 \$10.00

Volume 21 (1971) New Orleans.
GCAGS 021 \$15.00

Volume 22 (1972) Corpus Christi.

GCAGS 022 \$15.00

Volume 23 (1973) Houston.
GCAGS 023 \$20.00

Volume 24 (1974) Lafayette.
GCAGS 024 \$20.00

Volume 25 (1975) Jackson.
GCAGS 025 \$15.00

Volume 27 (1977) Austin.
GCAGS 027 \$25.00

Volume 29 (1979) San Antonio.
GCAGS 029 \$25.00

Volume 30 (1980) Lafayette.
GCAGS 030 \$30.00

Volume 31 with Supplement (1981)
Corpus Christi
GCAGS 031 \$10.00

Volume 32 (1982) Houston.
GCAGS 032 \$5.00

Volume 33 (1983) Jackson.
GCAGS 033 \$10.00

Volume 34 (1984) Shreveport.
GCAGS 034 \$10.00

Volume 35 (1985) Austin.
GCAGS 035 \$10.00

Volume 36 (1986) Baton Rouge.
GCAGS 036 \$5.00

Volume 37 (1987) San Antonio.
GCAGS 037 \$10.00

Volume 38 (1988) New Orleans.
GCAGS 038 \$30.00

Volume 39 (1989) Corpus Christi.
GCAGS 039 \$10.00

Volume 40 (1990) Lafayette.
GCAGS 040 \$40.00

Volume 41 (1991) Houston.
GCAGS 041 \$10.00

Volume 42 (1992) Jackson.
GCAGS 042 \$10.00

Volume 43 (1993) Shreveport.
GCAGS 043 \$10.00

Volume 44 (1994) Austin.
GCAGS 044 \$20.00

Volume 45 (1995) Baton Rouge.
GCAGS 045 \$40.00

Volume 46 (1996) San Antonio.
GCAGS 046 \$40.00

Volume 47 (1997) New Orleans.
GCAGS 047 \$40.00

Volume 48 (1998) Corpus Christi.
GCAGS 048 \$40.00

Volume 49 (1999) Lafayette.
GCAGS 049 \$60.00

Volume 50 (2000) Houston.
GCAGS 050 \$40.00 Book
GCAGS 050CD \$40.00 CD

Volume 51 (2001) Shreveport.
GCAGS 051 \$40.00 Book
GCAGS 051CD \$40.00 CD

Volume 52 (2002) Austin.
GCAGS 052 \$80.00 Book
GCAGS 052CD \$40.00 CD

Volume 53 (2003) Baton Rouge.
GCAGS 053 \$40.00 Book
GCAGS 053CD \$40.00 CD

Volume 54 (2004) San Antonio.
GCAGS 054 \$40.00 Book
GCAGS 054CD \$40.00 CD

Volume 55 (2005) New Orleans.
GCAGS 055 \$40.00 Book
GCAGS 055CD \$40.00 CD

Volume 56 (2006) Lafayette.
GCAGS 056 \$50.00 Book
GCAGS 056CD \$50.00 CD

Volume 57 (2007) Corpus Christi.
GCAGS 057 \$50.00 Book
GCAGS 057CD \$50.00 CD

Volume 58 (2008) Houston.
GCAGS 058 \$50.00 Book
GCAGS 058CD \$50.00 CD

Volume 59 (2009) Shreveport.
GCAGS 059 \$50.00 Book
GCAGS 059CD \$50.00 CD

Volume 60 (2010) San Antonio.
GCAGS 060 \$50.00 Book
GCAGS 060CD \$50.00 CD

Volume 61 (2011) Veracruz.
GCAGS 061 \$60.00 Book
GCAGS 061CD \$60.00 CD

Volume 62 (2012) Austin.
GCAGS 062 \$60.00 Book
GCAGS 062CD \$60.00 CD

Volume 63 (2013) New Orleans.
GCAGS 063 \$70.00 Book
GCAGS 063CD \$70.00 CD

Volume 64 (2014) Lafayette.
GCAGS 064 \$70.00 Book
GCAGS 064USB \$70.00 USB

Volume 65 (2015) Houston.
GCAGS 065 \$70.00 Book
GCAGS 065CD \$70.00 CD
GCAGS 065USB \$70.00 USB

Transactions 1951–2013 on DVD.
Papers and abstracts from Annual Meetings of
GCAGS from its first Annual
Meeting in 1951 through 2013
ISBN: 9781588610775.
GCAGS 996 \$290.00

SPONSORS

CHARGER EXPLORATION

Michael L. Jones
President/Geologist

Onshore Gulf Coast Prospect Generation and Consulting

1001 McKinney Street, Suite 801 Houston, TX 77002
Ofc: 713.654.0080 Cell: 713.398.3091
Email: mjones@chargerexploration.com
www.chargerexploration.com

Serving Corpus Christi for over 20 years



- We process 1st class mail with a direct discount to you
- No meter procedure change except for the amount you meter your envelopes

CALL 888-4332 for details - Ask for Anne

That old gas kick could be your next discovery!

Characterization of Unconventional Reservoirs

Traditional methods of core analysis cannot yield acceptable results when applied to unconventional reservoirs such as gas shales, tight gas sands, coals and thin bed formations.

Production controls on these reservoirs are not limited to hydrocarbons in place, permeability and porosity. Pay identification requires an understanding of complex lithologies and exotic mineralogies.

Only Core Lab offers the comprehensive range of unique technologies required to optimize your unconventional reservoirs.

Geological Petrophysical Geomechanical Geochemical



To learn more about our unique unconventional reservoir evaluation services contact Core Lab. (713) 328-2121 or (361) 289-5457 psinfo@corelab.com

© 2005 Core Laboratories. All rights reserved.

Case History

A comparison between methods that discriminate fluid content in unconsolidated sandstone reservoirs

Zhengyun Zhou¹ and Fred J. Hilterman²

ABSTRACT

Three seismic attributes commonly used to predict pore fluid and lithology are the fluid factor (ΔF), Poisson impedance (PI), and lambda-rho ($\lambda\rho$). We evaluated the pore-fluid sensitivity of these attributes with both well-log and seismic data in Tertiary unconsolidated sediments from the Gulf of Mexico where sand and shale are the only expected lithologies. While the sensitivity of one attribute versus another to discriminate pore fluid is often debated in the literature, the sensitivities of the three attributes are not independent but can be traced back to the fluid factor, which is a function of the P- and S-wave normal-incident reflection coefficients. Interestingly, the fluid factor, which is a reflectivity attribute, at the top of a hydrocarbon-saturated reservoir, is basically independent of the shale properties above the reservoir. It is a function of the brine and hydrocarbon impedances of the reservoir. The next attribute, Poisson impedance, is then

equal to the fluid factor times the sum of the brine and hydrocarbon impedances. Finally, the lambda-rho attribute is equal to the Poisson impedance multiplied by the same impedance sum. Essentially, the same scale factor differentiates these attributes, which does not significantly affect the sensitivity of the attributes. PI is the basis of the sensitivity for these attributes. As a means of testing their sensitivity for predicting pore fluid, we generated the three attributes along with their statistical distributions for different pore fluids for 183 reservoirs. The well-log statistical descriptions were then used to calibrate the seismic amplitude in a 3D survey to reflectivity values, thus allowing pore-fluid classification schemes based on Bayes' decision rules. In essence, seismic-amplitude quantification was based on regional statistics rather than individual wells within the 3D seismic survey to delineate the portions of the reservoir that were saturated with oil, gas, or brine.

INTRODUCTION

Pore-fluid and lithology predictions are two desired products in amplitude-versus-offset (AVO) analysis. To address pore-fluid prediction, [Smith and Gidlow \(1987\)](#) defined the fluid factor as the weighted difference between the reflectivities of P- and S-wave velocity. The weights came from mudrock equation ([Castagna, 1985](#)) or local measurements. In AVO gradient versus normal-incident P-wave (NIP) reflectivity crossplots, a brine-saturated (wet) sand falls closer to the mudrock line than the equivalent gas-saturated (gas) sand. Thus, the fluid factor would be near zero for a wet sand, while more negative for a gas sand. [Gidlow et al. \(1992\)](#) and [Fatti et al. \(1994\)](#) invert common-midpoint gathers for impedance reflectivity rather than P-wave and S-wave velocity reflectivity and redefined

the fluid factor as the weighted difference between the reflectivities of P-wave and S-wave impedance. Another AVO technique suggested by [Gray et al. \(1999\)](#) inverts for the reflectivity of rock properties, such as the Lamé coefficient (λ), shear rigidity (μ), and density (ρ).

The pore-fluid sensitivity of various AVO reflectivity attributes is discussed by [Castagna and Smith \(1994\)](#) and [Smith and Sutherland \(1996\)](#) based on data from 25 worldwide rock samples. Their results suggest that the fluid factor successfully distinguishes gas sands from wet sands for all AVO classes. Based on the same rock-property data, [Smith and Gidlow \(2000\)](#) compare the fluid factor with reflectivity attributes derived from λ , μ , and ρ . The fluid factor and Gray's suggested attributes are closely related and both are hydrocarbon indicators.

Prestack inversion ([Hampson, 1991](#); [Wallace and Young, 1996](#);

Presented by Fred Hilterman for Zhengyun Zhou in 2007 SEG Annual Meeting. Manuscript received by the Editor 19 January 2009; revised manuscript received 12 May 2009; published online 5 February 2010.

¹Formerly Center for Applied Geosciences and Energy, University of Houston, Houston, Texas, U.S.A.; presently Schlumberger, Houston, Texas, U.S.A. E-mail: zzhou7@slb.com.

²Geokinetics, Inc., Houston, Texas, U.S.A. E-mail: fred.hilterman@geokinetics.com.

© 2010 Society of Exploration Geophysicists. All rights reserved.

SPONSORS



Since 1905

Royal Exploration Company, Inc.

Bank of America

500 N. Shoreline Blvd. Suite 807 N
Corpus Christi, Texas 78471-1008

Alan Costello - Geologist Robert Rice - Geologist
Matt Hammer - Exploration Manager

Telephone: 361-888-4792 Fax: 361-888-8190

www.**GeoSteering**.com

281-573-0500
info@geosteering.com

Free introductory consultation
with modeling:
let us demonstrate whether
images or propagation resistivity
could add value to your well.

Personnel with degrees & 20+ years of oilfield experience

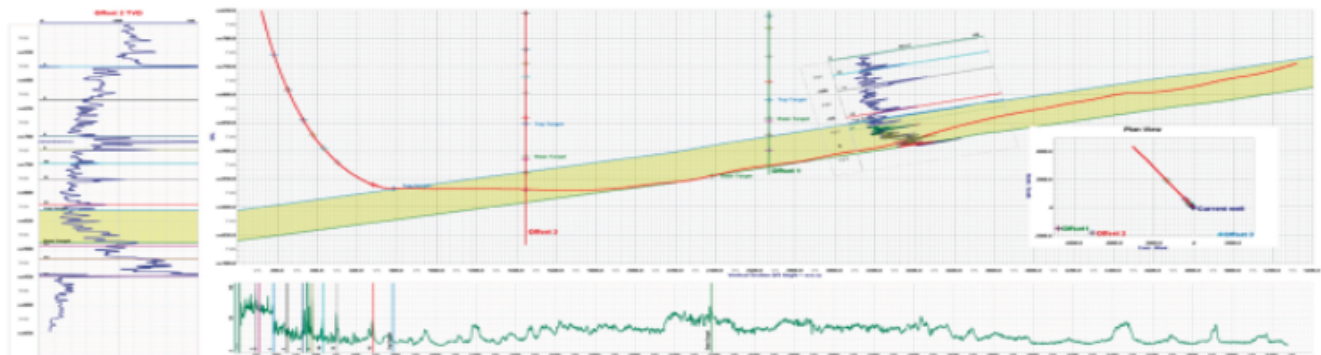
Proprietary software

TST interpretation for GR only jobs

**Image displays / interpretation for jobs with azimuthal GR,
resistivity or density**

**Resistivity modelling / interpretation for jobs with LWD
propagation resistivity**

Real-time (always)



Wallace and Young, 1997) extends the reflectivity domain to the impedance domain. Lambda-mu-rho, introduced by Goodway et al. (1997), was one of the main pore-fluid discriminators in the impedance domain. Goodway et al. (1997) observe that the data clusters for shale, wet sand, and gas sand have larger separations in the crossplot of $\lambda\rho$ versus $\mu\rho$ than in the crossplot of acoustic impedance (AI) versus shear impedance (SI). In addition, $\mu\rho$ helps to distinguish signatures of anomalous lithologies from hydrocarbon signatures. Many case histories (Besheli et al., 2004; Ojo et al., 2005; Larsen et al., 2006; Young and Tatham, 2007) were reported with applications of $\lambda\rho$ as a pore-fluid indicator.

Lambda-rho ($\lambda\rho$) is a weighted function of the acoustic and shear impedances; it is expressed as $\lambda\rho = (AI)^2 - 2(SI)^2$. Hilterman (2001) relates $\lambda\rho$ to the fluid-modulus term (Gassmann, 1951), assuming the dry-frame Poisson's ratio is approximately 0.125. However, $\lambda\rho$ does not always provide the maximum pore-fluid discrimination when the dry-frame properties of the rock vary. According to Russell et al. (2003), a better pore-fluid discriminator is obtained if the value two, the weight between $(AI)^2$ and $(SI)^2$, is changed slightly based on the dry-frame Poisson's ratio. After crossplotting attributes such as $\mu\rho$ versus $\lambda\rho$, a rotation into the pore-fluid projection axis (Hendrickson, 1999; Whitcombe and Fletcher, 2001) enhances the ability to discriminate with a single attribute. Quakenbush et al. (2006) rotated the AI-SI crossplot to its pore-fluid projection and related the new attribute to Poisson's ratio and density, and thus named it Poisson impedance (PI). While there are numerous AVO attributes for lithology and pore-fluid discrimination, most of them have a very strong link back to the fluid factor introduced by Smith and Gidlow (1987).

In this research, we first used an extensive well-log database to quantify and evaluate the pore-fluid sensitivity of the fluid factor, PI, and $\lambda\rho$ attributes for unconsolidated clastic sediments that are pre-

dominantly class 3 AVO anomalies. As a field validation of the well-log study, seismic AVO attributes were generated from a 3D survey. Then, the seismic attributes were calibrated using statistics derived from the well-log study, so that quantitative pore-fluid predictions can be made from the seismic attributes. Without sufficient well-log constraints within the actual 3D survey area, the fluid-factor reflectivity attribute is a better pore-fluid discriminator than PI or $\lambda\rho$ attributes.

WELL-LOG DATA

Seismic to borehole calibration equations, attributes, and statistical parameters were developed from 151 offshore Gulf of Mexico (GOM) wells selected from the study area in South Marsh Island (SMI). The rocks are unconsolidated clastic sediments from the Pleistocene to Miocene Periods. The general criteria for well selection were as follows:

- One well per lease block (approximately 25 km²)
- Minimum of 2000 m of logged data
- High-quality well-log curves including the self potential, gamma ray, neutron, density, sonic, shallow and deep resistivity, and caliper. Only a few shear-wave sonics were available and these were not included in the study.

Each suite of well-log curves was edited and intervals of questionable log values and intervals containing hydrocarbons were cataloged for future exclusion when rock-property statistics and seismic attributes were computed. A shale volume curve was generated for each well and then average P-wave slowness and density values at 60-m (200-ft) intervals were extracted for both brine-saturated (wet) sand reservoirs and their encasing shale. Data from a 60-m (200-ft) interval were considered a reservoir statistic if the interval had at least 9 m of density and velocity values for both sand and shale. Individual sand or shale beds with a thickness less than 3 m were excluded from the 60-m (200-ft) interval. Fluid substitution (Gassmann, 1951) for oil- and gas-saturated reservoir properties was conducted using fluid properties from Batzle and Wang (1992) and S-wave velocity estimates from Greenberg and Castagna (1992). Pore pressure and temperature for fluid substitution were taken from the well-log headers. Other fluid-substitution parameters were:

- API = 32
- Specific gas gravity = 0.7
- Salinity = 0
- Gas oil ratio (GOR) = maximum allowable GOR up to 1000 (scft/bbl)
- Water saturation = 30%

As an additional quality control, a sand reservoir was rejected if the ratio of the dry-frame bulk modulus to the shear modulus was not between 0.5 and 2.0. For the depth interval of seismic interest, 2900–3500 m (9500–11,500 ft), rock properties from 183 reservoirs were extracted to generate various seismic attributes and statistics.

Figure 1a and b show velocity and density values for the encasing shale and its respective sand layer with different reservoir pore fluids for the 183 reservoirs. To appreciate the difference between the encasing shale and the sand properties for each reservoir, we plot the wet-sand property along the abscissa and a specific reservoir's property on a vertical line. When the same sand and shale properties are displayed as depth trends (Figure 1c and d), significant differences

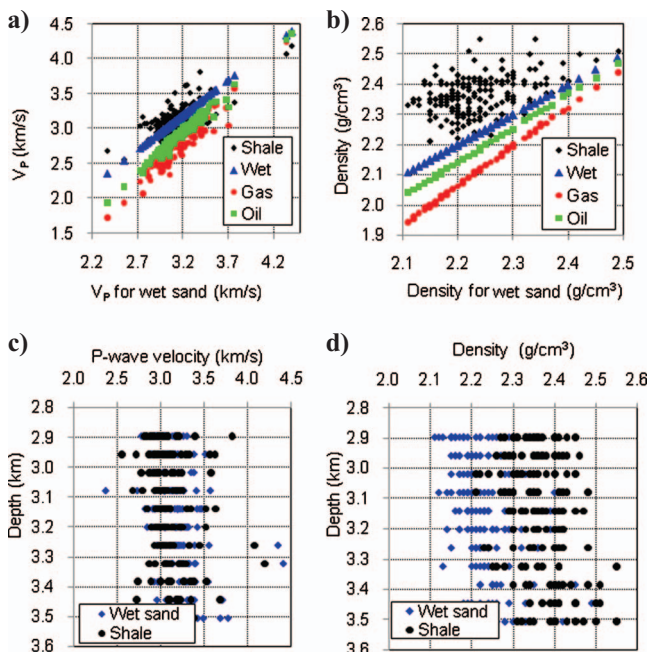



Figure 1. Crossplots of (a) P-wave velocity and (b) density values for encasing shale (black), wet (blue), oil (green), and gas (red) sands versus wet sand from 183 reservoirs in SMI. Depth trends are shown for (c) P-wave velocity and (d) density for wet sand (blue) and shale (black) from the same 183 reservoirs.

SPONSORS

An aerial black and white photograph of an industrial facility, likely a refinery or chemical plant. The site is filled with various structures, including large storage tanks, distillation columns, and piping. Numerous vehicles, including trucks and cars, are parked in a lot in the foreground. A tall crane is visible on the right side of the site. A large, stylized black fish logo is superimposed over the center of the image. The fish is facing right and has a curved body with a pointed tail. The background shows a flat landscape with some trees and a clear sky.

**SABALO
ENERGY**

SABALO ENERGY | P.O. BOX 2907 | CORPUS CHRISTI, TX 78403 | 361.888.7708 | SABALOENERGY.COM

between the wet-sand and shale properties are not obvious. For instance, while the encasing shale velocity in Figure 1a appears to be equally split between being faster and slower than its wet-sand reservoir; in Figure 1b, apparently, only 1% of the reservoirs have an encasing shale density that is lighter than the wet sand. This density relationship is not apparent from the density-depth trends for wet sand and shale as shown in Figure 1d.

In Figure 2a, NIP coefficients are plotted for shale over sand with brine-, oil-, and gas-saturation as blue, green, and red points, respectively. Similar to Figure 1a, Figure 2a is plotted with the wet-sand NIP for each reservoir along the abscissa. This allows one to quickly visualize the NIP difference between wet sand and its fluid-substituted hydrocarbon-saturated sand. There is significant correlation between the wet and hydrocarbon-saturated NIP values as expressed by the following relationships:

$$NIP_{oil} = -0.05 + 1.09NIP_{wet}, \quad R^2 = 0.94, \quad \text{and} \quad (1a)$$

$$NIP_{gas} = -0.09 + 1.14NIP_{wet}, \quad R^2 = 0.83, \quad (1b)$$

where, as noted in Table 1, NIP is the normal-incident P-wave reflection coefficient, and the subscripts refer to the reservoir pore-fluids. R^2 is a statistical measure as to how well a regression trend line approximates real data points.

For interpretation purposes, we crossplot the reservoirs' porosities versus the wet-sand NIP values in the upper portion of Figure 2a. In this study area, the wet-sand NIP values only have a slight correlation to porosity. This suggests that the velocity-porosity relationship

is controlled by sedimentation, which is often referred to as a depositional trend (Avseth, et al., 2005).

DEFINITION OF PORE-FLUID ATTRIBUTES

Fluid factor

Our interest is to derive rock-property statistics from the well-log curves to calibrate seismic attributes for a field in South Marsh Island that has both oil and gas reserves. At the same time, we are interested in determining if the seismic attributes are independent. The first attribute examined is the fluid-factor trace, which was defined by [Gidlow et al. \(1992\)](#) as

$$\Delta F(t) = NIP(t) - \gamma NIS(t), \quad (2)$$

where $NIP(t)$ and $NIS(t)$ are normal-incident traces associated with P-wave and S-wave reflections, respectively. The empirical weight γ minimizes $\Delta F(t)$ in brine-saturated reservoirs. When this occurs, the scalar γ is an estimate of $(NIP/NIS)_{wet}$. Of course, γ can be slowly varying both spatially and temporally. For a target reservoir, we assume γ is constant. Considering $NIS(t)$ is not particularly sensitive to the pore-fluid content, equation 2 becomes

$$\begin{aligned} \Delta F(t) &= NIP(t) - [(NIP/NIS)_{wet}]_{avg} NIS(t) \\ &\approx NIP(t) - NIP_{wet}(t), \end{aligned} \quad (3)$$

where $NIP(t)$ refers to the actual normal-incident trace with its cur-

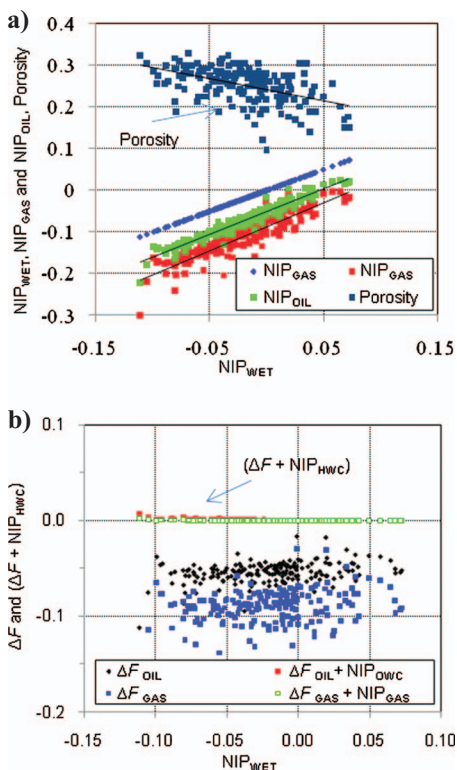
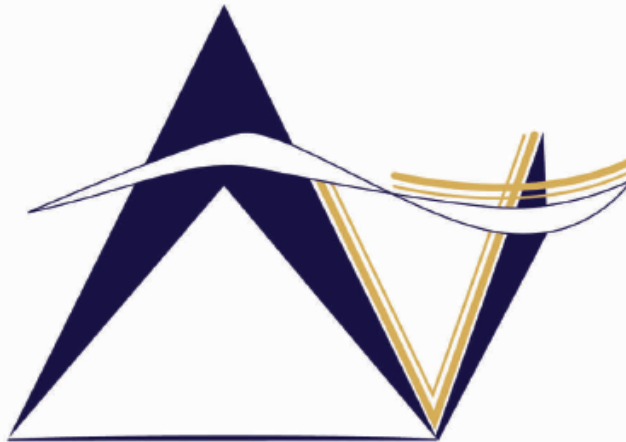


Figure 2. (a) Crossplot of NIP for wet, gas, and oil sands and porosity versus wet-sand NIP (porosity = $-0.53NIP_{wet} + 0.24$; $NIP_{oil} = 1.09NIP_{wet} - 0.05$; $NIP_{gas} = 1.14NIP_{wet} - 0.09$) and, (b) crossplot of fluid factor and summation of fluid factor and NIP from hydrocarbon-water contact for gas and oil sands versus wet-sand NIP.

Table 1. Symbol notation.

λ	Lamé coefficient lambda, or wavelength
μ	Shear rigidity
$\mu(\cdot), \sigma(\cdot)$	Mean and standard deviation
ρ	Density (rho)
α, β	P-wave and S-wave velocities
γ, γ_1	Weighting factors in ΔF and PI definition
θ	Incident angle
NIP, NIS	P-wave and S-wave normal-incident reflection coefficients
ΔF	Fluid factor, $NIP - \gamma NIS$
AI, SI	Acoustic and shear impedances
PI	Poisson impedance, $AI - \gamma_1 SI$
$R(\theta)$	Reflection coefficient at incident angle θ
$A(\theta)$	Seismic amplitude at incident angle θ
AP	Seismic amplitude at normal incidence for P-wave, $= K NIP$
AS	Seismic amplitude at normal incidence for S-wave, $= K NIS$
K, k	Constants between seismic amplitude and reflection coefficient, $K = k(4\pi b/\lambda)$ for thin bed
With ~ above	Property estimated from seismic data
Without ~ above	Theoretical property or property from well-log data
Subscripts: wet, oil, gas, hyd, hwc	Properties for brine, oil, gas, and hydrocarbon saturation, and from hydrocarbon-brine contact.

SPONSORS



VirTex Operating Company, Inc.

*615 North Upper Broadway, Suite 525, Corpus Christi, Texas 78477
(361) 882-3046*

SEI®

Seismic Exchange, Inc.

Strategic Speculative Surveys
Geophysical Data Marketing & Management

YOUR
Full Service
National
Seismic Data
Marketing Firm

Corpus Marketing Contact:
Beau Patrick

Corpus Office
361.884.2936

CORPUS CHRISTI DALLAS DENVER HOUSTON NEW ORLEANS TULSA

11050 Capital Park Dr., Houston, Texas 77041 832.590.5100

www.seismicexchange.com

rent pore fluid and $NIP_{wet}(t)$ refers to the same normal-incident trace if the pore fluid is brine. In theory then, when the reservoir is brine-saturated, $\Delta F(t)$ is zero, while if the reservoir is hydrocarbon-saturated, $\Delta F(t)$ becomes $[NIP_{hyd}(t) - NIP_{wet}(t)]$. In certain conditions, NIS_{wet} is zero or near zero, which causes the constant γ to be infinite by its definition of $(NIP/NIS)_{wet}$. However, this means the $NIS(t)$ trace is also zero, leaving the fluid factor equal to $NIP(t)$.

For the 183 reservoirs from South Marsh Island, ΔF , as specified by equation 3, is displayed for both gas- (blue squares) and oil-saturated sands (black dots) in the lower portion of Figure 2b. The magnitude of ΔF can be quantified to the pore-fluid properties through relationships similar to equation 1.

At the top of a hydrocarbon zone, the fluid factor can be expressed as (see Appendix A)

$$\begin{aligned}\Delta F_{hyd} &= (NIP_{hyd} - NIP_{wet}) \\ &= -NIP_{hwc} + (NIP_{hyd}NIP_{wet}NIP_{hwc}),\end{aligned}\quad (4)$$

where NIP_{hyd} and NIP_{wet} refer to the normal incidence at the interface of shale over hydrocarbon-saturated sand and shale over wet sand, respectively. NIP_{hwc} refers to the normal incidence at a hydrocarbon-water contact, such as an interface between the gas-saturated and brine-saturated portions of a reservoir. The second term on the right side in equation 4 is a higher-order term of NIP , and thus can be neglected. Then, the fluid factor at the top of a hydrocarbon-saturated zone is approximated as

$$\begin{aligned}\Delta F_{hyd} &\approx -NIP_{hwc} \\ &\approx \frac{AI_{hyd} - AI_{wet}}{AI_{hyd} + AI_{wet}},\end{aligned}\quad (5)$$

where AI is acoustic impedance and the subscripts hyd and wet refer

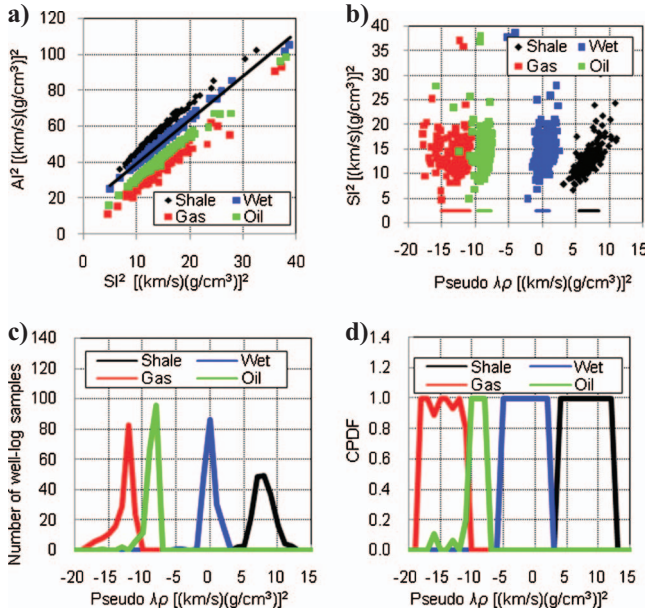


Figure 3. (a) Crossplot of AI^2 versus SI^2 , ($AI_{wet}^2 = 2.42SI_{wet}^2 + 15.44$); (b) crossplot of SI^2 versus pseudo-lambda-rho ($= AI^2 - 2.42SI^2 - 15.44$); (c) pseudo-lambda-rho histograms; and (d) pseudo-lambda-rho conditional probability density functions, CPDF, for shale (black), wet sand (blue), oil sand (green), and gas sand (red) from 183 reservoirs.

to hydrocarbon and brine saturation. Equation 5 indicates that ΔF is independent of the properties of the encasing medium and is only a function of the reservoir properties. The result of adding $[(NIP_{hyd} - NIP_{wet}) + NIP_{hwc}]$ for the 183 reservoirs as shown in Figure 2b is near-zero values when compared to the fluid factors plotted below them. Landrø (2001) had similar results for time-lapse studies. As shown by Wright (1986), NIP_{hwc} is always positive and the reflection amplitude increases with offset.

The shale beneath the reservoir might have different properties than the shale above the reservoir. However, if the NIP and NIS values for the lower and upper shale fall on the same wet trend curve (see example in Figure 2a), then the fluid factor for the reservoir bottom interface is the negative of the top-interface fluid factor. Thus, in an unconsolidated clastic basin, the fluid factor is normally independent of the shale properties above and below the sand reservoir.

Poisson impedance and $\lambda\rho$

Trace inversions of $NIP(t)$ and $NIS(t)$ yield the layer properties of acoustic impedance, $AI(t)$, and shear impedance, $SI(t)$. Quakenbush et al. (2006) defined the weighted difference between $AI(t)$ and $SI(t)$ as PI . The scale factor γ_1 in Poisson impedance is defined here as the average ratio between AI and SI in a wet zone, $[(AI/SI)_{wet}]_{avg}$, so that

$$\begin{aligned}PI(t) &= AI(t) - \gamma_1 SI(t) = AI(t) - [(AI/SI)_{wet}]_{avg} SI(t) \\ &\approx AI(t) - AI_{wet}(t),\end{aligned}\quad (6)$$

where $AI(t)$ refers to the actual acoustic impedance trace with its current pore fluid and $AI_{wet}(t)$ refers to the same acoustic impedance trace if the pore fluid is brine. Similar to the fluid factor, PI for a brine-saturated sand is close to zero; for an oil-saturated sand, it is negative; and, for a gas-saturated sand, more negative. Because seismic data lack low-frequency components, the actual impedance inversion often uses low-frequency AI and SI trends from available well-log or seismic interval-velocity control. Without well-log control, the estimated AI and SI from inversion may not reliably quantify PI .

If PI is multiplied by the background $(AI + \gamma_1 SI)$ and γ_1^2 is set to two, the AVO attribute becomes lambda-rho ($\lambda\rho$):

$$\begin{aligned}PI \times (AI + \gamma_1 SI) &= (AI - \gamma_1 SI)(AI + \gamma_1 SI) \\ &= AI^2 - \gamma_1^2 SI^2 = \lambda\rho, \quad \text{if } \gamma_1^2 = 2.\end{aligned}\quad (7)$$

In $\lambda\rho$, the difference term, $(AI - \gamma_1 SI)$ is much more sensitive to pore fluid and lithology than the summation term, $(AI + \gamma_1 SI)$. In this paper, we will follow a suggestion by Russell et al. (2003) and empirically estimate γ_1^2 to calculate a pseudo-lambda-rho, $\lambda\rho$, rather than accept a value of two for γ_1^2 . It is desirable to have the value of γ_1^2 set to the ratio AI^2/SI^2 for the brine-saturated reservoir, so that $\lambda\rho$ becomes

$$\begin{aligned}\tilde{\lambda\rho} &= AI^2 - \gamma_1^2 SI^2 = AI^2 - [(AI^2/SI^2)_{wet}]_{avg} SI^2 \\ &\approx AI^2 - AI_{wet}^2.\end{aligned}\quad (8)$$

PORE-FLUID ATTRIBUTES AT WELL-LOG RESOLUTION

Figure 3a shows the crossplot of AI^2 and SI^2 derived from the rock properties of the 183 reservoirs for shale and sand with brine, gas,

SPONSORS

STALKER ENERGY, L.P.

Austin Office:

1717 W. 6th Street, Ste 230

Austin, Texas 78703

512.457.8711

Contact: Bill Walker, Jr.

bwalker@stalkerenergy.com

Houston Office:

2001 Kirby Drive, Suite 950

Houston, Texas 77019

713.522.2733

Contact: Todd Sinex

tsinex@stalkerenergy.com

www.stalkerenergy.com



LMP PETROLEUM, INC.

EXPLORING SOUTH TEXAS

615 N. Upper Broadway
Suite 1770

Wells Fargo Bank Building
Corpus Christi, Texas 78401-0773

361-883-0923

Fax: 361-883-7102

E-mail: geology@lmpexploration.com

WELLSITE GEOSCIENCE SERVICES



**When time is money,
Wellsite Geoscience is
money well spent.**

Whether you're exploring a basin, producing a well or completing a shale play, time is money. That's why Weatherford Laboratories brings a suite of formation evaluation technologies right to the wellsite. Utilizing mud gas and cuttings, these technologies provide detailed data on gas composition, organic richness, mineralogy and chemostratigraphy in near real time. As a result, operators now have an invaluable tool to assist with sweet spot identification, wellbore positioning, completion design and hydraulic fracturing. We call it Science At the WellSite. You'll call it money well spent.

SCIENCE AT THE WELLSITE™

www.weatherfordlabs.com

Formation Evaluation | Well Construction | Completion | Production

©2013 Weatherford. All rights reserved.



and oil saturations. Linear trends are obvious for the plotted four categories (shale, wet, gas, and oil) because the S-wave velocity was predicted from the P-wave velocity using a linear equation. Equation 9a depicts the linear relation between AI^2 and SI^2 for wet sand. By rotating the coordinate axes to the wet-sand line, we obtain $\tilde{\lambda}\rho$ in equation 9b and illustrated it in Figure 3b.

$$AI^2 = 2.42SI^2 + 15.44, \tag{9a}$$

$$\tilde{\lambda}\rho = AI^2 - (2.42SI^2 + 15.44). \tag{9b}$$

The $\tilde{\lambda}\rho$ values have been translated by the scalar 15.44 so that the wet-sand attribute has a mean value of zero. The empirical factor γ_1^2 (Russell et al., 2003) in $\tilde{\lambda}\rho$ makes the slope of the four categories in Figure 3b more vertical than the factor two would. A standard deviation around the mean value (total length of two standard deviations) for each of the four categories is shown below the data clusters in Figure 3b. Figure 3c and d show the histograms and conditional probability density functions (CPDFs) (Duda et al., 2000) for $\tilde{\lambda}\rho$.

Figure 4a contains the crossplot of AI and SI for the same reservoirs used in Figure 3. Equation 10a linearly relates AI and SI for wet sand. Rotating the coordinate axes to the wet-sand line yields the PI attribute in equation 10b, which is illustrated in Figure 4b

$$AI = 1.34SI + 2.03, \tag{10a}$$

$$PI = AI - (1.34SI + 2.03). \tag{10b}$$

As was done for the $\tilde{\lambda}\rho$ attribute, the PI values have been translated so that the expected value of the PI attribute for wet-sand is zero. The breadth and position of the standard deviation lines below the four categories in Figure 4b are very similar in appearance to that observed for $\tilde{\lambda}\rho$ in Figure 3b. The PI histograms and CPDFs are plotted

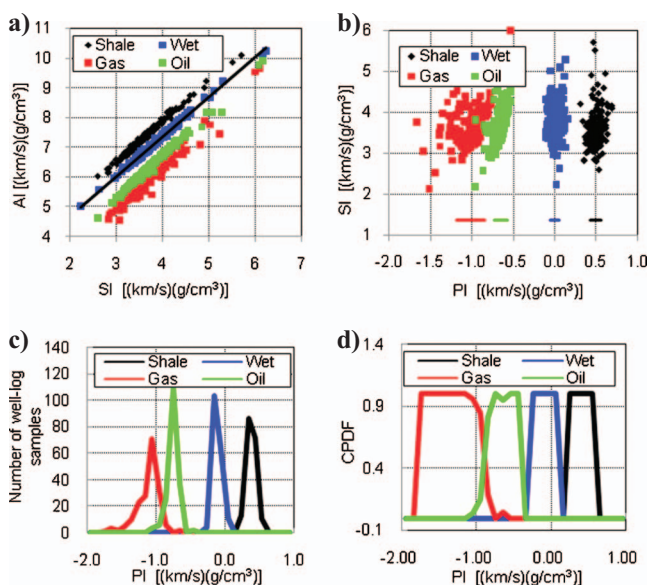


Figure 4. (a) Crossplot of AI versus SI, ($AI_{wet} = 1.34SI_{wet} + 2.03$); (b) crossplot of SI versus PI ($= AI - 1.34SI - 2.03$); (c) PI histograms; and (d) PI conditional probability density functions, CPDF, for shale (black), wet sand (blue), oil sand (green), and gas sand (red) from 183 reservoirs.

in Figure 4c and d. The PI classification of pore fluid will follow Bayes' decision rule (Avseth et al., 2005), which selects the classification with the maximum CPDF. This rule generates the PI classification criteria for pore fluid from Figure 4d as shown in Table 2.

NIP and NIS for shale over brine-, gas-, and oil-saturated sand were also calculated from the well-log database and are crossplotted in Figure 5a. Equation 11a quantifies the linear relationship between NIP and NIS for wet sand. Because the intercept of the wet-sand linear trend is not zero, an intercept term is included in the calculation of the fluid-factor ΔF in equation 11b:

$$NIP = 0.72NIS - 0.03, \tag{11a}$$

$$\Delta F = NIP - (0.72NIS - 0.03). \tag{11b}$$

Figure 5b shows the crossplot of NIS versus ΔF . For a wet-sand reflection, ΔF is close to zero, while for an oil-sand reflection, ΔF is negative, and for a gas-sand reflection, ΔF is more negative. The standard deviation lines in Figure 5b are broader with respect to the position of the clusters than observed either in Figures 3b or 4b. In fact, the position of the standard deviation lines for oil and gas overlap, indicating a difficulty in predicting oil from gas using the fluid factor. Figure 5c and d show histograms and CPDFs of ΔF for brine,

Table 2. Pore-fluid classification based on PI from well-log database.

Classification	PI range
Gas sand	$PI \leq -0.9$
Oil sand	$-0.9 < PI \leq -0.35$
Wet sand	$-0.35 < PI \leq 0.15$
Shale	$0.15 < PI$

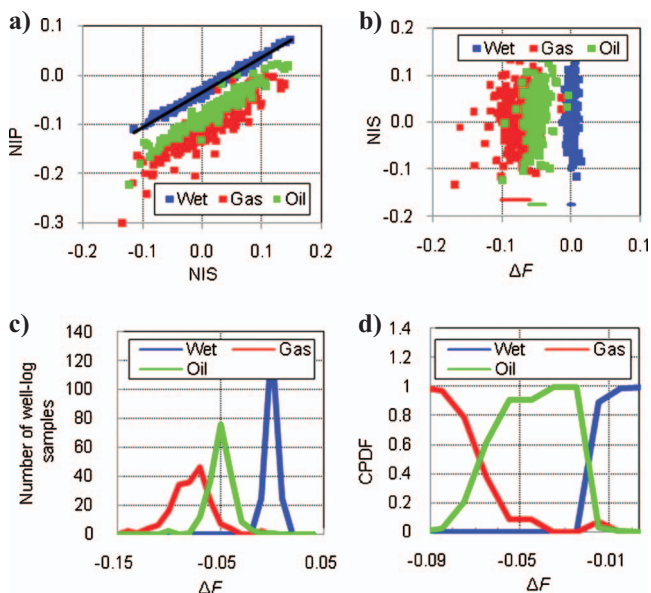
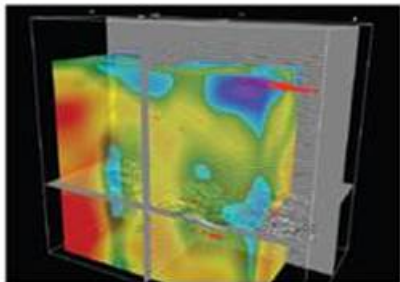


Figure 5. (a) Crossplot of NIP and NIS for shale over wet, oil, and gas saturations, ($NIP_{wet} = 0.72NIS_{wet} - 0.03$); (b) crossplot of NIS versus fluid factor ΔF ($= NIP - 0.72NIS + 0.03$); (c) ΔF histograms; and (d) ΔF CPDFs for wet (blue), oil (green), and gas sands (red).

SEIMAXSM
TECHNOLOGIES

Innovative Seismic
Processing Solutions



**2D and 3D Land and Marine
Pre-Stack Time and Depth Imaging**

**Pre- and Post-Stack Attributes
for Amplitude, Frequency and
Resolution**

4805 Westway Park Blvd. Houston, TX 77041
p: 832.554.4301 www.seimaxtech.com

oil, and gas saturation. From the CPDFs, Bayes' classification criteria for the fluid factor are shown in Table 3.

Sensitivity of pore-fluid attributes

Table 4 lists the mean and standard deviation values for the fluid factor, PI, and $\widetilde{\lambda\rho}$ attributes shown in Figures 3–5. The three attributes have different units and are normalized to compare their effectiveness for pore-fluid discrimination. The fluid factor and PI statistics were normalized to $\widetilde{\lambda\rho}$. After normalization, the gas standard deviation for PI is very close to that for $\widetilde{\lambda\rho}$, while the fluid-factor standard deviation is about 1.6 times that for $\widetilde{\lambda\rho}$ or PI. Based on Table 4, the PI sensitivity for pore-fluid discrimination is approximately the same as the $\widetilde{\lambda\rho}$ attribute and because of this, only the PI attribute is applied to field data.

Relationship between pore-fluid attributes

The fluid factor, PI, and $\widetilde{\lambda\rho}$ attributes are closely related. To illustrate this, let the acoustic impedance of a sand reservoir be AI and when the equivalent reservoir is brine-saturated the acoustic impedance is AI_{wet} . Also, let $\Delta AI = AI - AI_{wet}$ and $2AI = AI + AI_{wet}$, then the following holds

$$\text{Fluid Factor} \cong \Delta AI / 2AI = \Delta AI \times (2AI)^{-1}, \quad (12a)$$

$$PI = \Delta AI = \Delta AI \times (2AI)^0, \quad (12b)$$

$$\widetilde{\lambda\rho} = \Delta AI \times 2AI = \Delta AI \times (2AI)^1. \quad (12c)$$

Table 3. Pore-fluid classification based on fluid factor from well-log database.

Classification	ΔF range
Gas sand	$\Delta F \leq -0.066$
Oil sand	$-0.066 < \Delta F \leq -0.02$
Wet sand	$-0.02 < \Delta F$

Table 4. Mean and standard deviation for original and normalized fluid factor, PI and $\widetilde{\lambda\rho}$ from well-log database.

		Mean			Standard Deviation		
		Wet	Oil	Gas	Wet	Oil	Gas
Original	Fluid factor	0.000	-0.047	-0.080	0.005	0.013	0.021
	PI	0.00	-0.65	-1.01	0.06	0.08	0.17
	$\widetilde{\lambda\rho}$	0.00	-8.69	-12.99	0.98	1.00	2.07
Normalize to $\widetilde{\lambda\rho}$	Fluid factor	0.00	-7.66	-12.98	0.75	2.09	3.35
	PI	0.00	-8.36	-12.98	0.72	1.01	2.15
	$\widetilde{\lambda\rho}$	0.00	-8.69	-12.99	0.98	1.00	2.07

In short, the fluid factor, PI, and $\lambda\rho$ attributes consist of the sensitivity term ΔAI and the scalar term $2AI$, where the scalar term has a different exponent for each attribute. Thus, the sensitivity basis for these three attributes is mainly associated with ΔAI , PI. In fact, if the PI attribute from Figure 4, $PI = \frac{\Delta AI}{2AI} - 1.34SI + 2.03$, is substituted for AI_{wet} and the fluid factor and $\lambda\rho$ are recomputed using equations 12a and 12c, respectively, the results would be very similar to those observed in Figures 5b and 3b, respectively.

In the next section, the PI and fluid-factor statistics derived from regional wells near the study area are quantitatively applied to a 3D seismic survey for predicting the gas, oil, and brine portions of a reservoir.

SEISMIC DATA

Fairfield Industries provided the marine 3D seismic data for this study in SMI where the reservoir is located. Figure 6a depicts the time map of the reservoir horizon along with ten wells. The depth of the target zone is approximately 3000 m (10,000 ft). The wells had the following production status when the seismic survey was acquired. Wells 1 through 7 were abandoned oil wells and are indicated by black solid circles in Figure 6. Wells 8 and 9 are producing oil wells and are indicated by purple solid circles, while Well 10 is a producing gas well and is indicated by a red star. The reservoir is located beneath a major fault which accounts for the distorted time image as shown by comparing the time map (Figure 6a) to the depth map developed from the ten wells (Figure 6b).

SEISMIC ATTRIBUTES

Fluid factor from seismic data

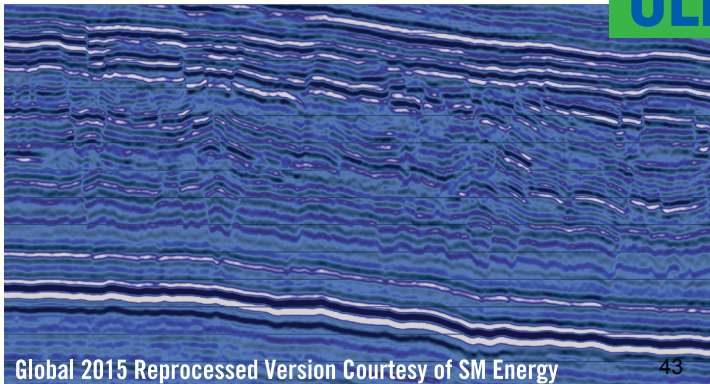
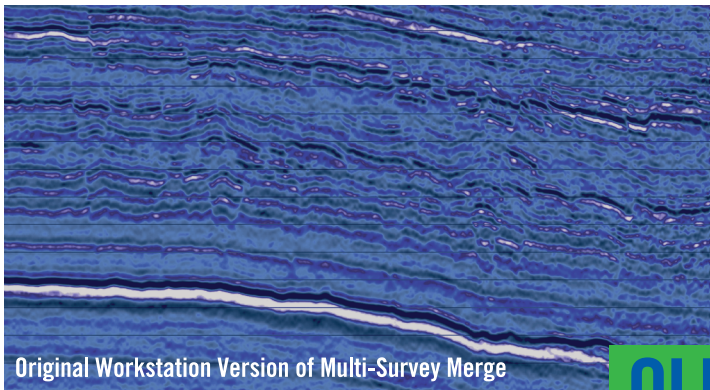
Smith and Gidlow's (1987) linear approximation of Zoeppritz's equation is

$$RC(\theta) = \frac{1}{2} \left(\frac{\Delta\alpha}{\alpha} + \frac{\Delta\rho}{\rho} \right) \frac{1}{\cos^2 \phi} - \frac{4\beta^2}{\alpha^2} \left(\frac{\Delta\beta}{\beta} + \frac{\Delta\rho}{\rho} \right) \sin^2 \phi - \frac{1}{2} \frac{\Delta\rho}{\rho} \left(\tan^2 \phi - \frac{4\beta^2}{\alpha^2} \sin^2 \phi \right), \quad (13)$$

where $RC(\theta)$ is the reflection coefficient at incident angle θ , α is the average P-wave velocity of the upper and lower media, β is the average S-wave velocity, ρ is the average density, Δ is the difference of rock properties (lower medium properties minus upper), and ϕ is the average of the incident and transmitted angles. By dropping the higher-order terms and assuming $\alpha = 2\beta$ and $\phi = \theta$, equation 13 yields

$$RC(\theta) = NIP / \cos^2 \theta - 2NIS \times \sin^2 \theta. \quad (14)$$

If the reflection coefficients at two different incident angles, $RC(\theta_1)$ and $RC(\theta_2)$, are available,



Recent innovations in technology and understanding have started a quiet revolution in seismic processing. Reprocessing vintage 3D seismic using Global's new work flows can bring new life to your old data in a fast, affordable, and actionable way. To the geoscientist, this means:

- Increased bandwidth and higher resolution
- Better imagery; sharper, crisper, better positioned fractures & faults
- Insanely flat gathers in both offset and azimuth, out to 50° of incidence angles
- More accurate offset amplitudes in the final gathers, producing true "Inversion Ready Gathers"
- New, interesting azimuthal characterizations of the seismic data producing new attributes which correlate nicely to well production data

OLD DATA. NEW RESULTS.

These "Inversion Ready Gathers" produce more accurate traditional rock properties and lithology predictions, and when combined with the new azimuthal attributes, ambient seismic, and also existing well production and engineering information, allow for predictions of hydrocarbon production at both existing and proposed well- and even stage-level locations. The ability to predict production away from the well in an accurate fashion enables optimization of all phases of your field development program in both conventional and unconventional reservoirs.

REVEAL NEW VALUE IN YOUR DATA
www.globalgeophysical.com/REPROCESS or
Contact REPROCESS@globalgeophysical.com



then NIP and NIS are derived as (Zhou and Hilterman, 2007)

$$NIP = \frac{RC(\theta_1)\cos^2 \theta_1 \sin^2 2\theta_2 - RC(\theta_2)\cos^2 \theta_2 \sin^2 2\theta_1}{\sin^2 2\theta_2 - \sin^2 2\theta_1}, \quad (15a)$$

and

$$NIS = \frac{2[RC(\theta_1)\cos^2 \theta_1 - RC(\theta_2)\cos^2 \theta_2]}{\sin^2 2\theta_2 - \sin^2 2\theta_1}. \quad (15b)$$

Conventional seismic angle-stacks provide amplitudes, $A(\theta)$, rather than reflection coefficients, $RC(\theta)$. Lin and Phair (1993) expressed the seismic amplitude for a thin bed as

$$A(\theta) = k \frac{4\pi b}{\lambda} RC_{top}(\theta) \cos(\theta_{tr}), \quad (16)$$

where $A(\theta)$ is the thin-bed seismic amplitude at incident angle θ , k is a constant value (can be considered a data-processing scalar), b is the thin-bed thickness, λ is the wavelength in the thin bed ($b < \lambda/8$), $RC_{top}(\theta)$ is the reflection coefficient from the upper boundary, and θ_{tr} is the transmitted angle. For a single seismic survey, k and λ can be considered constants, especially when we focus on a target reservoir. Assuming the bed thickness, b , does not change for the target reservoir, equation 16 can be written as

$$A(\theta) = K \times RC(\theta) \cos(\theta), \quad (17)$$

where $K = k \times (4\pi b/\lambda)$ and the incident and transmitted angles are assumed equal. If we replace the reflection coefficient $RC(\theta)$ with the amplitude $A(\theta)/\cos(\theta)$ in equations 15a and 15b, then we get

$$\begin{aligned} AP &= \frac{\frac{A(\theta_1)}{\cos \theta_1} \cos^2 \theta_1 \sin^2 2\theta_2 - \frac{A(\theta_2)}{\cos \theta_2} \cos^2 \theta_2 \sin^2 2\theta_1}{\sin^2 2\theta_2 - \sin^2 2\theta_1} \\ &= K \times NIP, \end{aligned} \quad (18a)$$

and

$$AS = \frac{2 \left[\frac{A(\theta_1)}{\cos \theta_1} \cos^2 \theta_1 - \frac{A(\theta_2)}{\cos \theta_2} \cos^2 \theta_2 \right]}{\sin^2 2\theta_2 - \sin^2 2\theta_1} = K \times NIS, \quad (18b)$$

where, as noted in Table 1, AP and AS are the seismic thin-bed responses at normal incidence for P- and S-wave reflections.

Horizon maps for the target reservoir were generated from the near-angle stack (10°) and the far-angle stack (30°), and then equations 18a and 18b were applied to obtain the AP and AS maps shown in Figure 6c and d. As noted in Table 1, a symbol representing a property derived from seismic field data has a tilde (\sim) above it, while theoretical properties do not have a tilde.

From additional well control, it is known that the target reservoir is brine-saturated in the northern part of the study area (enclosed by the dashed blue box in Figure 6c and d). The color-bar scales associated with the horizon amplitude maps indicate the existence of the constant K because reflection coefficients are between ± 1 . To calculate the seismic fluid factor and make a quantitative prediction of saturation, K needs to be estimated and removed from \widetilde{AP} and AS. In

this paper, we applied a normalization method to convert the seismic amplitudes AP and AS into normal-incident values NIP and NIS as were developed from the well-log data.

Normalization to the unit normal (Johnson and Leone, 1964) is defined as

$$u_i = \frac{x_i - \mu(\mathbf{x})}{\sigma(\mathbf{x})}, \quad (19)$$

where u_i is the normalized value of the data sample x_i , which is assumed to have a normal distribution, and μ and σ are the mean and standard deviation of data set \mathbf{x} . Equation 19 then can be rewritten as

$$y_i = u_i \sigma(\mathbf{y}) + \mu(\mathbf{y}). \quad (20)$$

where \mathbf{y} is another data set. Equations 19 and 20 convert data x_i into a unit normal distribution u_i , and then into the statistical distribution of the data y_i . In our study, we converted seismic amplitudes into normal-incident reflection coefficients. As an example, using the attribute NIP, we have

$$\widetilde{NIP}_i = \frac{\widetilde{AP}_i - \mu(\widetilde{AP})}{\sigma(\widetilde{AP})} \sigma(\widetilde{NIP}) + \mu(\widetilde{NIP}), \quad (21)$$

where $\mu(\widetilde{AP})$ and $\sigma(\widetilde{AP})$ are the mean and standard deviation of \widetilde{AP} from the seismic data, while $\mu(\widetilde{NIP})$ and $\sigma(\widetilde{NIP})$ are the mean and standard deviation of the NIP derived from well-log data. A key point here is how to calculate the mean and standard deviation of seismic and well-log data.

Figure 7a and b show the histograms of NIP and NIS for gas, oil, and wet sand that were derived from the well-log data. From these two figures, the gas-sand NIP histogram in Figure 7a is more negative than the wet-sand histogram, while the three pore-fluid histograms in Figure 7b for NIS overlap each other. The reason for the relative position of the histograms is that the S-wave velocity, V_s , does not change appreciably with saturation, while P-wave velocity, V_p , does. Similar histogram relationships can be seen in Figure 7c and d, which are for the seismic amplitudes, AP and AS, using data from

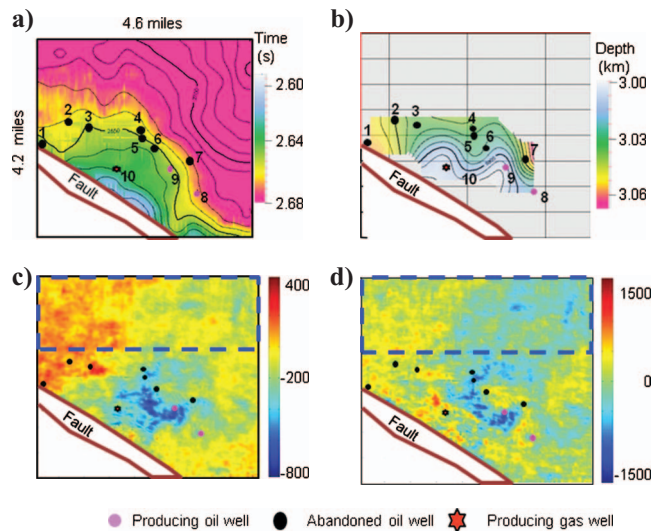


Figure 6. (a) Structural time map of reservoir horizon; (b) depth map from available ten wells; and normal-incident seismic-amplitude maps (c) \widetilde{AP} , and (d) AS generated from angle stacks using equation 18a and 18b.

the whole survey and data from the assumed wet area in the northern part of the survey. The AS histogram curve from the assumed wet area is in the center of the histogram curve from the whole survey (Figure 7d), while the AP histogram from the assumed wet area is slightly more positive than the histogram from the whole survey (Figure 7c). Table 5 shows the mean and standard deviation values for the well-log and seismic histograms.

There are two options for applying the normalization equation. The first option is to consider AP and AS as having separate mean and standard deviation values for each of the three subsets that identify the pore-fluid state. With option 1, equations 22a and 22b normalize AP and AS to normal-incident reflection coefficients:

$$\widetilde{NIP}_i^{(1)} = \left[\frac{\widetilde{AP}_i - \mu(\widetilde{AP}_{wet})}{\sigma(\widetilde{AP}_{wet})} \right] \sigma(NIP_{wet}) + \mu(NIP_{wet}), \quad (22a)$$

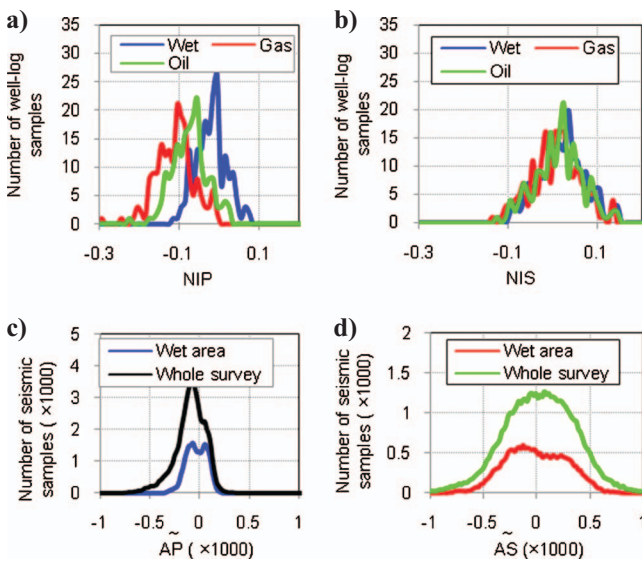


Figure 7. Histograms of (a) NIP and (b) NIS for wet (blue), oil (green), and gas (red) reservoirs based on well-log data. Histograms from seismic-amplitude maps are plotted for (c) AP and (d) AS from whole survey and assumed wet area in the northern part of the 3D survey.

Table 5. Mean and standard deviation values for NIP and NIS from well-log data and AP and AS from seismic data.

		P-wave		S-wave	
		Mean (μ)	Standard deviation (σ)	Mean (μ)	Standard deviation (σ)
NIP or NIS	Wet	-0.02	0.038	0.021	0.0527
	Wet, oil, and gas	-0.068	0.0568	0.014	0.0536
\widetilde{AP} or \widetilde{AS}	Wet	-32.25	102.28	-9.29	287.17
	All survey	-95.21	153.13	26.18	346.27

$$\widetilde{NIS}_i^{(1)} = \left[\frac{\widetilde{AS}_i - \mu(\widetilde{AS}_{wet})}{\sigma(\widetilde{AS}_{wet})} \right] \sigma(NIS_{wet}) + \mu(NIS_{wet}), \quad (22b)$$

where $\widetilde{NIP}_i^{(1)}$ and $\widetilde{NIS}_i^{(1)}$ are estimates of NIP and NIS from normalized AP and AS. \widetilde{AP}_{wet} and \widetilde{AS}_{wet} represent seismic amplitudes from the brine-saturated portions of the survey. NIP_{wet} and NIS_{wet} are NIP and NIS well-log values for brine-saturated reservoirs. The superscript (1) indicates that option 1 for normalization is being computed. Equations 22a and 22b relate to brine saturation; similar expressions exist when the pore fluid is oil or gas. The histogram distributions of NIP shift significantly when the saturation is changed from gas, oil, and brine, and thus the mean values for each pore-fluid case are significantly different (Figure 7a). To apply equations 22a and 22b exactly, the mean and standard deviations for seismic data that are brine-, oil-, and gas-saturated are required. However, the saturation state for the entire seismic survey is unknown, because the objective of the study was to determine the boundaries of the gas and oil reservoirs. Thus, in this first option, it is difficult to accurately normalize AP and AS for the whole survey to the well-log data scale of $\widetilde{NIP}_i^{(1)}$ and $\widetilde{NIS}_i^{(1)}$. So we generated normalization equations according to seismic data from the assumed wet area in the northern part and the wet-sand NIP and NIS data from the well logs. The normalization equations (equations 22a and 22b) are then applied to the whole data set. Because different mean and standard deviation values are applied to AP and to AS, the relative ratio between AP and AS is not maintained during normalization. The ratio after normalization tends to be similar to the ratio between NIP and NIS for the wet-sand properties from the well-log curves. This option can help to reduce scaling errors introduced during processing.

Figure 8a and b show the estimated $NIP^{(1)}$ and $NIS^{(1)}$ maps after applying the first option of normalization, equations 22a and 22b. Figure 8c shows a crossplot of $NIP^{(1)}$ versus $NIS^{(1)}$ values from Figure 8a and b. The application of the linear relationship between $NIP^{(1)}$ and $NIS^{(1)}$ in the assumed wet area is given in equation 23a. Equation 23b provides the fluid factor based on equation 23a.

$$\widetilde{NIP}^{(1)} = 0.66\widetilde{NIS}^{(1)} - 0.034, \quad R^2 = 0.84, \quad (23a)$$

$$\widetilde{\Delta F}^{(1)} = \widetilde{NIP}^{(1)} - (0.66\widetilde{NIS}^{(1)} - 0.034). \quad (23b)$$

Because a horizon map has been used to determine the relationship between $NIP^{(1)}$ and $NIS^{(1)}$ rather than a seismic section of traces, it is possible to include an intercept value, which will normalize the wet-sand values to a zero mean (Simm et al., 2000). The application of equation 23b to the maps in Figure 8a and b yields the fluid-factor map shown in Figure 8d. The classification criteria in Table 3, which are based on well-log data, are applied to the fluid-factor map, and the predicted pore-fluid map with time contours is shown in Figure 8e and with depth contours in Figure 8f.

The second normalization option is to consider AP and AS as having the same scale factor from well-log data. Equations 24a and 24b are the normalization equations applied for AP and AS.

$$\widetilde{NIP}_i^{(2)} = \frac{\widetilde{AP}_i - \mu(\widetilde{AS}_{ALL})}{\sigma(\widetilde{AS}_{ALL})} \sigma(\text{NIS}_{ALL}) + \mu(\text{NIS}_{ALL}), \quad (24a)$$

$$\widetilde{NIS}_i^{(2)} = \frac{\widetilde{AS}_i - \mu(\widetilde{AS}_{ALL})}{\sigma(\widetilde{AS}_{ALL})} \sigma(\text{NIS}_{ALL}) + \mu(\text{NIS}_{ALL}), \quad (24b)$$

where \widetilde{AS}_{ALL} is \widetilde{AS} from the whole seismic survey. NIS_{ALL} is the NIS derived by combining the data of brine-, gas- and oil-saturation from well-log data. In Figure 7b, the NIS histograms for various water saturations are very similar. Thus, we can generate the normalization equation based on \widetilde{AS} from the whole survey and NIS for the combination of the data of gas, oil, and wet sands from the well-log database. The normalization equation is then applied to both \widetilde{AP} and \widetilde{AS} . This second option maintains the relative ratio between \widetilde{AP} and \widetilde{AS} . Figure 9a and b contain the $\widetilde{NIP}^{(2)}$ and $\widetilde{NIS}^{(2)}$ maps after applying option 2 normalization, which is equation 24.

Figure 9c shows the crossplot derived from the $\widetilde{NIP}^{(2)}$ and $\widetilde{NIS}^{(2)}$ maps. The linear equation between $\widetilde{NIP}^{(2)}$ and $\widetilde{NIS}^{(2)}$ for the area assumed to be brine saturated is given in equation 25a. Equation 25b provides the fluid factor based on equation 25a:

$$\widetilde{NIP}^{(2)} = 0.33\widetilde{NIS}^{(2)} + 0.0022, \quad R^2 = 0.84, \quad (25a)$$

$$\widetilde{\Delta F}^{(2)} = \widetilde{NIP}^{(2)} - (0.33\widetilde{NIS}^{(2)} + 0.0022). \quad (25b)$$

The subsequent fluid-factor map for option 2 is shown in Figure 9d. The well-log classification criteria in Table 3 are applied to the seismic fluid-factor map, and the predicted pore-fluid map with time contours is shown in Figure 9e and with depth contours in Figure 9f.

In the final classification maps (Figures 8e, 8f, 9e, and 9f), red refers to gas sand; green, oil sand; and, blue, wet sand. In Figure 8e and f, the classification for wells 1, 2, 3, 8, and 10 matches the known well production, while others do not. With regard to the producing wells, the classification of two of the three wells matches the known production. In Figure 9e and f, the classification of wells 1, 2, 3, 8, 9, and 10 matches the known well production. The classification of all three producing wells matches the known production. In both Figures 8 and 9, the depth maps correlate better than the time maps with the pore-fluid contacts from the classification schemes. In short, option 2 for normalizing the seismic amplitude to the normal-incident scale produced a better classification scheme based on the known production from the wells and based on the similarity of pore-fluid contact boundaries with the depth contours.

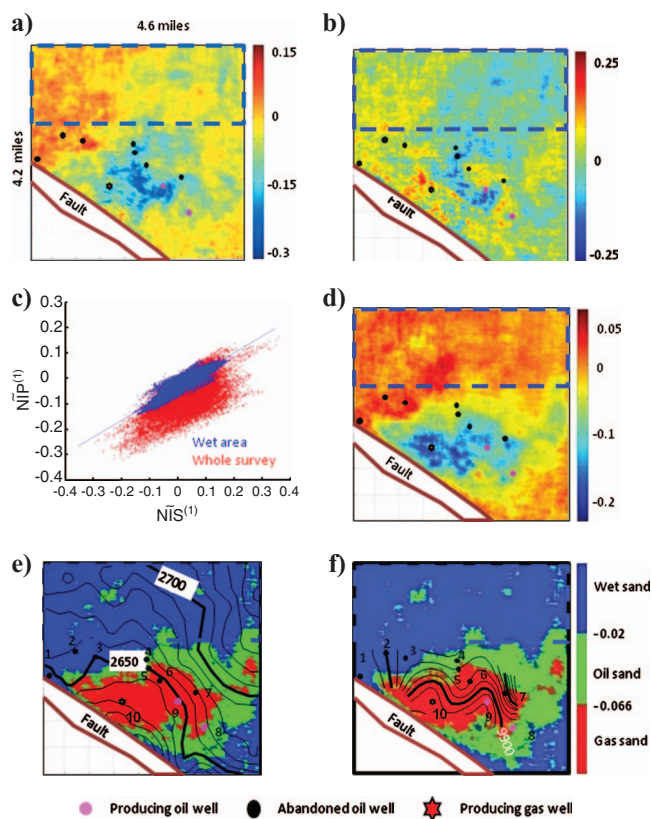


Figure 8. (a) $\widetilde{NIP}^{(1)}$ map and (b) $\widetilde{NIS}^{(1)}$ map after applying Option 1 of the normalization methods to AP and AS maps; (c) crossplot of $\widetilde{NIP}^{(1)}$ versus $\widetilde{NIS}^{(1)}$ from map values in (a) and (b) for the whole survey area and for the assumed wet area. The linear equation, $\widetilde{NIP}^{(1)} = 0.66\widetilde{NIS}^{(1)} - 0.034$, is based on the wet area. The fluid-factor $\widetilde{\Delta F}^{(1)}$ map (d) is based on the linear equation in (c). The final classification maps are obtained by applying Table 3 to the map in (d) and then overlaying with time contours (e) and depth contours (f) from well picks.

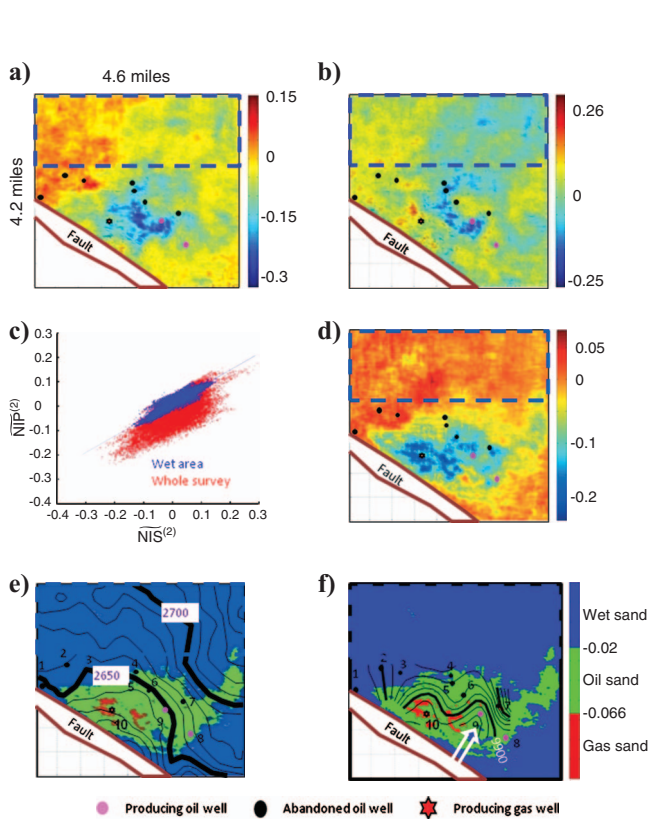


Figure 9. (a) $\widetilde{NIP}^{(2)}$ map and (b) $\widetilde{NIS}^{(2)}$ map after applying option 2 of the normalization methods to AP and AS maps; (c) crossplot of $\widetilde{NIP}^{(2)}$ versus $\widetilde{NIS}^{(2)}$ from map values in (a) and (b) for the whole survey area and for the assumed wet area. The linear equation, $\widetilde{NIP}^{(2)} = 0.33\widetilde{NIS}^{(2)} + 0.0022$, is based on the wet area. The fluid-factor $\widetilde{\Delta F}^{(2)}$ map (d) is based on the linear equation in (c). The final classification maps are obtained by applying Table 3 to the map in (d) and then overlaying with time contours (e) and depth contours (f) from well picks.

PI from seismic data

Seismic wavelets were estimated from reflections around the reservoir for three angle-stack volumes. However, even though numerous wells were located within the 3D survey area, none of the wells had both density and velocity logs through the reservoir zone to con-

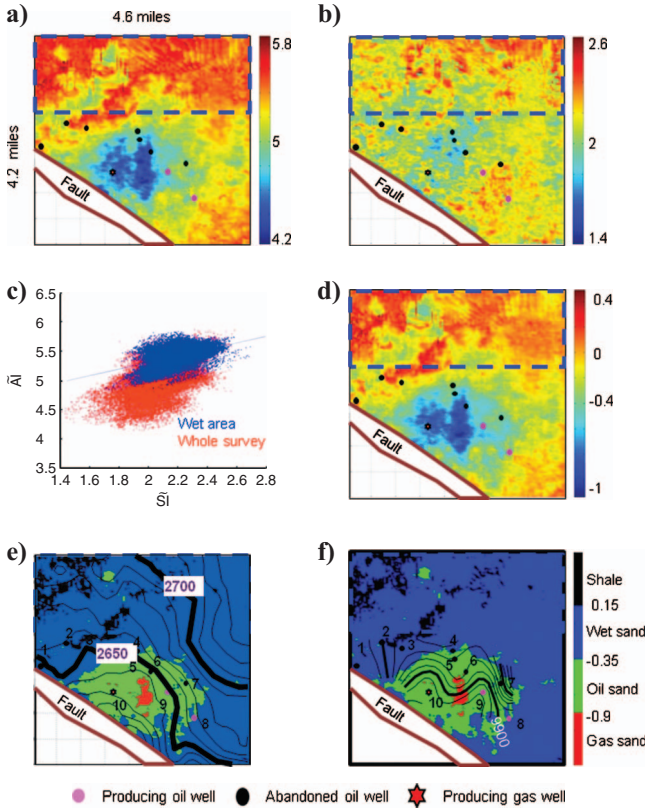


Figure 10. Horizon maps for (a) acoustic impedance (\tilde{AI}) and (b) shear impedance (\tilde{SI}) after inversion of seismic angle stacks in SMI; (c) crossplot of AI versus SI from (a) and (b). The wet area is assumed to be the dashed box area in the northern portion of the maps in (a) and (b). The linear equation, $AI = 0.56SI + 4.18$, is based on the wet area. The Poisson impedance PI map (d) is based on the linear equation in (c). The final classification maps are obtained by applying Table 2 to the map in (d) and then overlaying with time contours (e) and depth contours (f) from well picks.

trol the wavelet estimate or the initial low-frequency trends. A single linear low-frequency trend was finally used for the initial AI and another for SI. The three angle-stack volumes were simultaneously inverted for AI and SI (Tonellot et al., 2001). Figure 10a and b shows the acoustic impedance (AI) and shear impedance (SI) maps for the target horizon. Theoretically, because the inversion method yields properly scaled impedances, no scale normalization is needed. Figure 10c shows the crossplot of AI versus SI map values for the area assumed to be brine-saturated and for the whole survey area. The linear relation given in equation 26a between AI and SI in the wet area provides the PI in equation 26b.

$$\tilde{AI} = 0.56\tilde{SI} + 4.18, \quad R^2 = 0.21, \quad (26a)$$

$$\tilde{PI} = \tilde{AI} - (0.56\tilde{SI} + 4.18). \quad (26b)$$

The classification criteria in Table 2 were applied to the PI map in Figure 10d to yield the pore-fluid classification maps with time contours shown in Figure 10e, and with depth contours shown in Figure 10f. The color identification scheme for all sands is the same as the one in Figure 9e and f, while black is introduced to refer to shale. In general, the classification of wells 1, 2, 3, 4, and 9 matches the known well production, while the others do not. The classification of one of the two oil producing wells matches the known production. Unfortunately, the classification of the gas well is not correct. In Figure 10e, neither the gas-oil contact nor the oil-water contact correlates to the time contours. In Figure 10f, the gas-oil contact does not correlate to the depth contours, but the oil-water contact has a limited correlation to the depth contours. The pore-fluid classification from the fluid-factor map in Figure 9f is considered better than the PI classification in Figure 10f.

DISCUSSION

The rock properties derived from the well-log curves do not vary in the depth range of 2900–3500 m (9500–11,500 ft). To test possible statistical variations, the depth range was divided into two parts, 2900–3200 m (9500–10,500 ft) and 3260–3500 m (10,700–11,500 ft). Then, every sample and every other sample to every fifth sample were selected to form new subsets. Table 6 lists the mean and standard deviation values for these subsets. The difference of the mean and standard deviation for each set from the original data set is also shown in Table 6. The statistical differences caused by depth are in the same order of magnitude as the differences caused by alternating

Table 6. Mean and standard deviation (std) values of NIP and NIS from difference subsets of SMI well-log data set.

	Sample skipped	NIP		NIP difference		NIS		NIS difference	
		Mean	Std	Mean	Std	Mean	Std	Mean	Std
2900–3500 m (9500–11500 ft)	0	-0.0199	0.038	0	0	-0.0475	0.0501	0	0
	1	-0.0178	0.0388	0.0021	0.0008	-0.044	0.0508	0.0035	0.0007
	2	-0.0207	0.0395	-0.0008	0.0015	-0.0489	0.0509	-0.0014	0.0008
	3	-0.0154	0.0421	0.0045	0.0041	-0.0394	0.0543	0.0081	0.0042
	4	-0.0111	0.0387	0.0088	0.0007	-0.0376	0.0518	0.0099	0.0017
2900–3200 m (9500–10500 ft)	0	-0.0244	0.0383	-0.0045	0.0003	-0.053	0.0498	-0.0055	-0.0003
3260–3500 m (10700–11500 ft)	0	-0.011	0.036	0.0089	-0.002	-0.0365	0.0492	0.011	-0.0009

the samples selected. So in our field example, the statistical variation within the selected depth interval can be neglected.

In Figure 8f, five of 10 wells match with the known production, which includes two of the three producing wells. The northern part of the gas-oil contact is consistent with the depth contours from the well picks. No depth contours are available to evaluate the oil-water contact.

In Figure 9f, six of 10 wells match with the known production, which includes all three of the producing wells. The northern part of oil-water contact is consistent with the depth contours. The classification indicates a gas cap in the western part of the structure.

In Figure 10f, four of ten wells match with the known production, which includes one of three producing wells. The oil-water contact is consistent with the depth contours, while the gas-oil contact is inconsistent with the depth contours. A possible reason is that impedance inversion without well control to accurately estimate the seismic wavelets or provide initial impedance trends gives unreliable results for AI and SI.

Because the fluid content at the abandoned wells may not be totally brine-saturated, the producing wells are better to evaluate the success of the three methods. In general, the pore-fluid classification based on the fluid factor with option 2 normalization, $\Delta F^{(2)}$ in Figure 9f is better than the fluid-factor prediction with option 1 normalization $\Delta F^{(1)}$ in Figure 8f, which is better than PI pore-fluid prediction in Figure 10f.

Because the problem of determining partial gas-saturated reservoirs from fully saturated reservoirs was not an objective of this research, it is not unreasonable to expect that the procedures outlined in this study would have the potential to quantify water saturation. We have illustrated techniques to differentiate the fluid factor of a fully saturated gas reservoir from the fluid factor of an oil-saturated reservoir and the fluid factor for a partial gas-saturated reservoir is close to that for an oil-saturated reservoir. Solving the partial gas-saturation problem with quantification techniques similar to those presented in this study is definitely worthy of future investigation.

The linear trends of the rock properties displayed in Figures 1–5 must be viewed with some reservations as the S-wave velocity for sand and shale were estimated using linear expressions of the P-wave velocity and lithologic content. While these transformations are considered to be fairly robust, crossplot examples from Castagna et al. (1998) illustrate the magnitude of scatter that can be expected when actual laboratory measurements of S-wave velocity are used in seismic attributes rather than empirical and/or theoretical estimates.

Results from this study indicate areas for future research such as predicting thin-bed reservoir thickness from the amplitude of the fluid-factor response. As noted previously, the fluid factors from the top and bottom interfaces of a hydrocarbon-saturated reservoir are approximately $(-NIP_{\text{hwc}})$ and NIP_{hwc} , respectively, if the lithologies (shale, limestone, etc.) above and below the reservoir are the same. While the NIP reflection coefficients for gas-saturated sands vary from -0.3 to 0.0 in Figure 5a, the fluid factor is much more stable with a value of approximately -0.09 (Figure 5b). A thin bed can have different NIP values for the top and bottom reservoir interfaces making the thickness of a reservoir difficult to predict from the seismic response. However, the fluid factor, once calibrated for a local area as was done in Figure 5b, can be treated as a constant leaving the bed thickness (in two-way time) as the main variable in the seismic amplitude. Note, to some extent, the porosity of the sand can vary from prospect to prospect in the local area and the thickness can still be estimated from the fluid factor.

CONCLUSIONS

We compare three AVO attributes, fluid factor, PI, and $\tilde{\lambda\rho}$ from their definitions to examples from well-log data and seismic data. These three AVO attributes are closely related. For a shale/sand sequence with no unexpected lithologies present such as coal or limestone, even though the fluid factor is theoretically derived from the difference of two reflectivities from the top interface of a very thick reservoir, it is independent of the medium properties above the interface if we neglect an insignificant higher-order term of reflectivity. As such, the fluid factor equals the negative of the normal-incident reflection coefficient generated at a hydrocarbon-water contact having properties derived from the reservoir.

PI which theoretically reduces to $AI - AI_{\text{wet}}$, is also the basis for the sensitivity measurements of pseudo-lambda-rho and the fluid factor. The difference between these three attributes is the power of the scalar term, $(AI + AI_{\text{wet}})$, that is then multiplied with PI. From our interpretation of the well-log histograms in this class 3 AVO environment, PI has essentially the same pore-fluid discrimination as $\lambda\rho$.

In the SMI field example, the fluid-factor attribute yielded a better pore-fluid classification than PI based on a rather subjective validation. Without robust well control, the PI attributes lose their advantage over the fluid factor for pore-fluid discrimination. The results for $\lambda\rho$ would be similar to the PI results. We apply normalization technology of seismic-amplitude maps to normal-incident maps. This exercise was an attempt to quantify the amplitude on reflectivity maps similar to the quantification of impedance maps.

Crossplotting attribute values from horizon maps can provide linear relationships between attributes such as AI and SI rather than just ratios. This additional term, the intercept, allows a translation of the estimated brine-saturated values of the attribute to near-zero values.

ACKNOWLEDGMENTS

We would like to thank Geokinetics Inc. for the rock-property database and Fairfield Industries for the 3D seismic data in the study area. Support for this study comes from the sponsors of the Reservoir Quantification Laboratory at the University of Houston. In addition, portions of this work were prepared with the partial support of DOE under Grant No. DE-FC26-04NT15503. The authors are indebted to Jon Downton, George Smith, Steve Arcone, two anonymous editors, and a reviewer for their helpful suggestions to clarify various points in the article. However, any errors in opinions, findings, conclusions or recommendations expressed herein are those of the authors.

APPENDIX A

RELATIONSHIP BETWEEN FLUID-FACTOR AND FLUID-CONTACT REFLECTIONS

At the top of a hydrocarbon reservoir, the fluid factor is expressed as

$$\Delta F_{\text{hyd}} = NIP_{\text{hyd}} - NIP_{\text{wet}}, \quad (\text{A-1})$$

where the subscripts hyd and wet refer to hydrocarbon and brine saturation.

The proof of equation 4 is easily shown by introducing a new parameter, e :

$$\Delta F_{\text{hyd}} = \text{NIP}_{\text{hyd}} - \text{NIP}_{\text{wet}} = -\text{NIP}_{\text{hwc}} + e. \quad (\text{A-2})$$

Then,

$$e = \text{NIP}_{\text{hyd}} - \text{NIP}_{\text{wet}} + \text{NIP}_{\text{hwc}}. \quad (\text{A-3})$$

The NIP terms in equation A-3 are then expressed in terms of their respective acoustic impedances, AI, to yield

$$e = \frac{\text{AI}_{\text{hyd}} - \text{AI}_{\text{shale}}}{\text{AI}_{\text{hyd}} + \text{AI}_{\text{shale}}} - \frac{\text{AI}_{\text{wet}} - \text{AI}_{\text{shale}}}{\text{AI}_{\text{wet}} + \text{AI}_{\text{shale}}} + \frac{\text{AI}_{\text{wet}} - \text{AI}_{\text{hyd}}}{\text{AI}_{\text{wet}} + \text{AI}_{\text{hyd}}}. \quad (\text{A-4})$$

Equation A-4 can also be written as

$$e = \frac{A - B + C}{(\text{AI}_{\text{hyd}} + \text{AI}_{\text{shale}})(\text{AI}_{\text{wet}} + \text{AI}_{\text{shale}})(\text{AI}_{\text{wet}} + \text{AI}_{\text{hyd}})}, \quad (\text{A-5})$$

where

$$A = (\text{AI}_{\text{hyd}} - \text{AI}_{\text{shale}})(\text{AI}_{\text{wet}} + \text{AI}_{\text{shale}})(\text{AI}_{\text{wet}} + \text{AI}_{\text{hyd}}), \quad (\text{A-6})$$

$$B = (\text{AI}_{\text{hyd}} + \text{AI}_{\text{shale}})(\text{AI}_{\text{wet}} - \text{AI}_{\text{shale}})(\text{AI}_{\text{wet}} + \text{AI}_{\text{hyd}}), \quad (\text{A-7})$$

$$C = (\text{AI}_{\text{hyd}} + \text{AI}_{\text{shale}})(\text{AI}_{\text{wet}} + \text{AI}_{\text{shale}})(\text{AI}_{\text{wet}} - \text{AI}_{\text{hyd}}). \quad (\text{A-8})$$

Inserting equations A-6–8 into the numerator of equation A-5 and rearranging yields

$$A - B + C = (\text{AI}_{\text{hyd}} - \text{AI}_{\text{shale}})(\text{AI}_{\text{wet}} - \text{AI}_{\text{shale}}) \times (\text{AI}_{\text{wet}} - \text{AI}_{\text{hyd}}). \quad (\text{A-9})$$

Substituting equation A-9 into equation A-5, we obtain

$$e = \frac{(\text{AI}_{\text{hyd}} - \text{AI}_{\text{shale}})(\text{AI}_{\text{wet}} - \text{AI}_{\text{shale}})(\text{AI}_{\text{wet}} - \text{AI}_{\text{hyd}})}{(\text{AI}_{\text{hyd}} + \text{AI}_{\text{shale}})(\text{AI}_{\text{wet}} + \text{AI}_{\text{shale}})(\text{AI}_{\text{wet}} + \text{AI}_{\text{hyd}})} = \text{NIP}_{\text{hyd}}\text{NIP}_{\text{wet}}\text{NIP}_{\text{hwc}}. \quad (\text{A-10})$$

Combining equations A-2 and 10 yields equation A-11, which is the same as equation 4:

$$\Delta F_{\text{hyd}} = \text{NIP}_{\text{hyd}} - \text{NIP}_{\text{wet}} = -\text{NIP}_{\text{hwc}} + (\text{NIP}_{\text{hyd}}\text{NIP}_{\text{wet}}\text{NIP}_{\text{hwc}}). \quad (\text{A-11})$$

REFERENCES

- Avseth, P., T. Mukerji, and G. Mavko, 2005, Quantitative seismic interpretation — Applying rock physics tools to reduce interpretation risk: Cambridge University Press.
- Batzle, M. and Z. Wang, 1992, Seismic properties of pore fluids: *Geophysics*, **57**, 1396–1408.
- Besheli, S. A., S. S. Hendi, and J. Vali, 2004, LMR — A robust reservoir

- properties indicator in carbonate reservoirs, EAGE, Extended Abstracts.
- Castagna, J. P., M. L. Batzle, and R. L. Eastwood, 1985, Relationships between compressional-wave and shear-wave velocities in clastic silicate rocks: *Geophysics*, **50**, 571–581.
- Castagna, J. P., and S. W. Smith, 1994, Comparison of AVO indicators: A modeling study: *Geophysics*, **59**, 1849–1855.
- Castagna, J. P., H. W. Swan, and D. J. Foster, 1998, Framework for AVO gradient and intercept interpretation: *Geophysics*, **63**, 948–956.
- Duda, R. O., P. E. Hart, and D. G. Stork, 2000, Pattern classification: John Wiley & Sons.
- Fatti, J., G. Smith, P. Vail, P. Strauss, and P. Levitt, 1994, Detection of gas in sandstone reservoirs using AVO analysis: A 3-D seismic case history using the geostack technique: *Geophysics*, **59**, 1362–1376.
- Gassmann, F., 1951, Über die elastizität poroser medien: *Vierteljahrsschr. Der Soc. Petr. Eng. J.*, **1**, 235–248.
- Gidlow, P. M., G. C. Smith, and P. J. Vail, 1992, Hydrocarbon detection using fluid factor traces, a case study: How useful is AVO analysis?: Joint SEG/EAEG summer research workshop, SEG/EAEG, Technical Program and Abstracts, 78–89.
- Goodway, B., T. Chen, and J. Downton, 1997, Improved AVO fluid detection and lithology discrimination using Lamé petrophysical parameters; “ $\lambda\rho$,” “ $\mu\rho$,” & “ λ/μ ,” fluid stack, from P and S inversions: 67th Annual International Meeting, SEG, Expanded Abstracts, 183–186.
- Gray, D., B. Goodway, and T. Chen, 1999, Bridging the gap: using AVO to detect changes in fundamental elastic constants: 69th Annual International Meeting, SEG, Expanded Abstracts, 852–855.
- Greenberg, M. L. and J. P. Castagna, 1992, Shear-wave estimation in porous rocks: Theoretical formulation, preliminary verification and applications: *Geophysical Prospecting*, **40**, 195–210.
- Hampson, D., 1991, AVO inversion, theory and practice: *The Leading Edge*, **10**, 39–42.
- Hendrickson, J. S., 1999, Stacked: *Geophysical Prospecting*, **47**, 663–706.
- Hilterman, F. J., 2001, Seismic amplitude interpretation: Distinguished Instructor Series: SEG/EAGE, 4.
- Johnson, N. L. and F. C. Leone, 1964, Statistics and experimental design in engineering and the physical sciences: John Wiley & Sons.
- Landrø, M., 2001, Discrimination between pressure and fluid saturation changes from time-lapse seismic data: *Geophysics*, **66**, 836–844.
- Larsen, T. H., C. Ojo, and S. Gemelli, 2006, Lambda-Rho processing — A tool to reveal full hydrocarbon potentials: EAGE, Extended Abstracts.
- Lin, T. L. and R. Phair, 1993, AVO Tuning: 63rd Annual International Meeting, SEG, Expanded Abstracts, 727–730.
- Ojo, C., P. Licalsi, S. Gemelli, M. Atkins, and T. Larsen, 2005, Lambda-Rho processing — A tool to reveal full hydrocarbon potentials: Onshore Nigeria interpretation and drilling case history: 75th Annual International Meeting, SEG, Expanded Abstracts, 1315–1318.
- Quakenbush, M., B. Shang, and C. Tuttle, 2006, Poisson impedance: *The Leading Edge*, **25**, 128–138.
- Russell, B. H., K. Hedlin, and F. J. Hilterman, 2003, Fluid-property discrimination with AVO: A Biot-Gassmann perspective: *Geophysics*, **68**, 29–39.
- Simm, R., R. White, and R. Uden, 2000, The anatomy of AVO crossplots: *The Leading Edge*, **19**, 150–155.
- Smith, G. C., and P. M. Gidlow, 1987, Weighted stacking for rock property estimation and detection of gas: *Geophysical Prospecting*, **35**, 993–1014.
- Smith, G. C., and P. M. Gidlow, 2000, A comparison of the fluid factor with λ and μ in AVO analysis: 70th Annual International Meeting, SEG, Expanded Abstracts, 122–125.
- Smith, G. C., and R. A. Sutherland, 1996, The fluid factor as an AVO indicator: *Geophysics*, **61**, 1425–1428.
- Tonellot, T., D. Macé, and V. Richard, 2001, Joint stratigraphic inversion of angle-limited stacks: 71st Annual International Meeting, SEG, Expanded Abstracts, 227–230.
- Wallace, R., and R. Young, 1996, Pre-stack inversion: Evolving the science of inversion: *CSEG Recorder*, **21**, 10, 3–3.
- Wallace, R., and R. Young, 1997, Prestack inversion: an extension of AVO for lithology and hydrocarbon fluid quantification: 67th Annual International Meeting, SEG, Expanded Abstracts, 1541–1543.
- Whitcombe, D. N., and J. G. Fletcher, 2001, The AIGI cross plot as an aid to AVO analysis and calibration: 71st Annual International Meeting, SEG, Expanded Abstracts, 219–222.
- Wright, J., 1986, Reflection coefficients at pore-fluid contacts as a function of offset: *Geophysics*, **51**, 1858–1860.
- Young, K. T., and R. H. Tatham, 2007, Lambda-mu-rho inversion as a fluid and lithology discriminator in the Columbus Basin Offshore Trinidad: 77th Annual International Meeting, SEG, Expanded Abstracts, 214–217.
- Zhou, Z., and F. J. Hilterman, 2007, Is there a basis for AVO attributes: 77th Annual International Meeting, SEG, Expanded Abstracts, 244–248.

Corpus Christi Geological Society Papers available for purchase at the Texas Bureau of Economic Geology

Note: Publication codes are hyperlinked to their online listing in [The Bureau Store](http://begstore.beg.utexas.edu/store/) (<http://begstore.beg.utexas.edu/store/>).

Cretaceous-Wilcox-Frio Symposia, D. B. Clutterbuck, Editor, 41 p., 1962.
[CCGS 002S](#) \$15.00

Type Logs of South Texas Fields, Vol. I, Frio Trend. Compiled by Don Kling. Includes 134 fields. 158 p., 1972. Ring binder.
[CCGS 015TL](#) \$25.00

Type Logs of South Texas Fields, Vol. II, Wilcox (Eocene) Trend. Compiled by M. A. Wolbrink. 98 p., 1979. Ring binder.
[CCGS 016TL](#) \$25.00

Field Trip Guidebooks

South Texas Uranium. J. L. Cowdrey, Editor. 62 p., 1968.
[CCGS 102G](#) \$12.00

Hidalgo Canyon and La Popa Valley, Nuevo Leon, Mexico. CCGS 1970 Spring Field Conference. 78 p., 1970.
[CCGS 103G](#) \$8.00

Padre Island National Seashore Field Guide. R. N. Tench and W. D. Hodgson, Editors. 61 p., 1972.
[CCGS 104G](#) \$5.00

Triple Energy Field Trip, Uranium, Coal, Gas—Duval, Webb & Zapata Counties, Texas. George Faga, Editor. 24 p., 1975.
[CCGS 105G](#) \$10.00

Minas de Golondrinas and Minas Rancherías, Mexico. Robert Manson and Barbara Beynon, Editors. 48 p. plus illus., 1978.
[CCGS 106G](#) \$15.00

Portrero Garcia and Huasteca Canyon, Northeastern Mexico. Barbara Beynon and J. L. Russell, Editors. 46 p., 1979.
[CCGS 107G](#) \$15.00

Modern Depositional Environments of Sands in South Texas. C. E. Stelling and J. L. Russell, Editors. 64 p., 1981.
[CCGS 108G](#) \$15.00

Geology of Peregrina & Novillo Canyons, Ciudad Victoria, Mexico, J. L. Russell, Ed., 23 p. plus geologic map and cross section, 1981.
[CCGS 109G](#) \$10.00

Geology of the Llano Uplift, Central Texas, and Geological Features in the Uvalde Area. Corpus Christi Geological Society Annual Spring Field Conference, May 7-9, 1982. Various paginated. 115 p., 53 p.
[CCGS 110G](#) \$15.00

Structure and Mesozoic Stratigraphy of Northeast Mexico, prepared by numerous authors, variously paginated. 76 p., 38 p., 1984.
[CCGS 111G](#) \$15.00

Geology of the Big Bend National Park, Texas, by C. A. Berkebille. 26 p., 1984.
[CCGS 112G](#) \$12.00

GEO LINK POST

<http://www.lib.utexas.edu/books/landsapes/index.php> Free service. Rare, fragile, hard-to-find, public domain documents covering various topics about the landscape of Texas. Includes the Texas Geological Survey from 1887 until 1894.

USGS TAPESTRY OF TIME AND TERRAIN <http://tapestry.usgs.gov> The CCGS is donating to all of the 5th and 6th grade schools in the Coastal Bend. Check it out--it is a spectacular map. You might want to frame one for your own office. The one in my office has glass and a metal frame, and It cost \$400 and it does not look as good as the ones we are giving to the schools.

FREE TEXAS TOPOS'S <http://www.tnris.state.tx.us/digital.htm> these are TIFF files from your state government that can be downloaded and printed. You can ad them to SMT by converting them first in Globalmapper. Other digital data as well.

FREE NATIONAL TOPO'S [http://store.usgs.gov/b2c_usgs/b2c/start/\(xcm=r3standardpitrex_prd\)/.do](http://store.usgs.gov/b2c_usgs/b2c/start/(xcm=r3standardpitrex_prd)/.do) go to this webpage and look on the extreme right side to the box titled TOPO MAPS DOWNLOAD TOPO MAPS FREE.

<http://www.geographynetwork.com/> Go here and try their top 5 map services. My favorite is 'USGS Elevation Date.' Zoom in on your favorite places and see great shaded relief images. One of my favorites is the Great Sand Dunes National Park in south central Colorado. Nice Dunes.

<http://antwrp.gsfc.nasa.gov/apod/asropix.html> Astronomy picture of the day--awesome. I click this page everyday.

<http://www.spacimaging.com/gallery/ioweek/iow.htm> Amazing satellite images. Check out the gallery.

<http://www.ngdc.noaa.gov/seg/topo/globegal.shtml> More great maps to share with kids and students.

www.ccgeo.org Don't forget we have our own we page.

<http://terra.nasa.gov/gallery/> Great satellite images of Earth.

www.ermaper.com They have a great free downloadable viewer for TIFF and other graphic files called ER Viewer.

<http://terrasrver.com> Go here to download free aerial photo images that can be plotted under your digital land and well data. Images down to 1 meter resolution, searchable by Lat Long coordinate. Useful for resolving well location questions.

TYPE LOGS OF SOUTH TEXAS FIELDS by Corpus Christi Geological Society

NEW (2009-2010)TYPE LOGS IN RED; ***2011;**

lost now found

ARANSAS COUNTY

Aransas Pass/McCampbell Deep
Bartell Pass
Blackjack
Burgentine Lake
Copano Bay, South
Estes Cove
Fulton Beach
Goose Island
Half Moon Reef
Nine Mile Point
Rockport, West
St. Charles
Tally Island
Tract 831-G.O.M. (offshore)
Virginia

BEE COUNTY

Caesar
Mosca
Nomanna
Orangedale(2)
Ray-Wilcox
San Domingo

Tulsita Wilcox

Strauch_Wilcox

BROOKS COUNTY

Ann Mag
Boedecker
Cage Ranch
Encintas
ERF
Gyp Hill

Gyp Hill West

Loma Blanca
Mariposa
Mills Bennett
Pita
Tio Ayola
Tres Encinos

CALHOUN COUNTY

Appling
Coloma Creek, North
Heyser
Lavaca Bay
Long Mott
Magnolia Beach
Mosquito Point
Olivia
Panther Reef
Powderhorn
Seadrift, N.W.
Steamboat Pass
Webb Point
S.E. Zoller

CAMERON COUNTY

Holly Beach
Luttes
San Martin (2)
Three Islands, East

Vista Del Mar

COLORADO COUNTY

E. Ramsey
Graceland N. Fault Bik
Graceland S. Fault Bik

DEWITT COUNTY

Anna Barre
Cook
*******Nordheim**
Smith Creek
Warmley

Yorktown, South

DUVAL COUNTY

DCR-49
Four Seasons
Good Friday
Hagist Ranch
Herbst
Loma Novia
Petrox
Seven Sisters
Seventy Six, South
Starr Bright, West

GOLIAD COUNTY

Berclair
North Blanca
Bombs
Boyce
Cabeza Creek, South
Goliad, West
St Armo

HIDALGO COUNTY

Alamo/Donna
Donna
Edinburg, West
Flores-Jeffress
Foy
Hidalgo

LA Blanca

McAllen& Pharr
McAllen Ranch
Mercedes
Monte Christo, North
Penitas
San Fordyce
San Carlos
San Salvador
S. Santallana
Shary
Tabasco
Weslaco, North
Weslaco, South

JACKSON COUNTY

Carancahua Creek
Francitas
Ganado & Ganado Deep
LaWard, North
Little Kentucky

Maurbro

StewartSwan Lake

Swan Lake, East
Texana, North
West Ranch

JIM HOGG COUNTY

Chaparosa
Thompsonville,N.E.

JIM WELLS COUNTY

Freebom
Hoelsher
Palito Blanco

Wade City

KARNES COUNTY

Burnell
Coy City
Person
Runge

KENEDY COUNTY

Candelaria
Julian
Julian, North
Laguna Madre

Rita

Stillman

KLEBERG COUNTY

Alazan
Alazan, North
Big Caesar
Borregos
Chevron (offshore)
Laguna Larga
Seeligson
Sprint (offshore)

LA SALLE COUNTY

*****Pearsall**

LAVACA COUNTY

Hallettsville
Hope
Southwest Speaks
Southwest Speaks Deep
LIVE OAK COUNTY

Atkinson

Braslau

Chapa

Clayton

Dunn

Harris

Houdman

Kittie West-Salt Creek

Lucille

Sierra Vista

Tom Lyne

White Creek

White Creek, East

MATAGORDA COUNTY

Collegeport

MCMULLEN COUNTY

Arnold-Weldon

Brazil

Devil's Waterhole

Hostetter

Hostetter, North

NUECES COUNTY

Agua Dulce (3)

Arnold-David

Arnold-David, North

Baldwin Deep

Calallen

Chapman Ranch

Corpus Christi, N.W.

Corpus Christi West C.C.

Encinal Channel

Flour Bluff/Flour Bluff, East

GOM St 9045(offshore)

Indian Point

Mustang Island

Mustang Island, West

Mustang Island St.

889S(offshore)

Nueces Bay/Nueces Bay

West

Perro Rojo

Pita Island

Ramada

Redfish Bay

Riverside

Riverside, South

Saxet

Shield

Stedman Island

Turkey Creek

REFUGIO COUNTY

Bonnieview/Packery Flats

Greta

La Rosa

Lake Pasture

Refugio, New

Tom O'Connor

SAN PATRICIO COUNTY

Angelita East

Commonwealth

Encino

Enos Cooper

Geronimo

Harvey

Hiberia

Hodges

Mathis, East

McCampbell Deep/Aransas Pass

Midway

Midway, North

Odem

Plymouth

Portilla (2)

Taft

Taft, East

White Point, East

STARR COUNTY

El Tanque

Garcia

Hinde

La Reforma, S.W.

Lyda

Ricaby

Rincon

Rincon, North

Ross

San Roman

Sun

Yturria

VICTORIA COUNTY

Helen Gohike, S.W.

Keeran, North

Marcado Creek

McFaddin

Meyersville

Placedo

WEBB COUNTY

Aquilares/Glen Martin

Big Cowboy

Bruni, S.E.

Cabezon

Carr Lobo

Davis

Hirsch

Juanita

Las Tiendas

Nicholson

O'Hem

Olmitos

Tom Walsh

WHARTON COUNTY

Black Owl

WILLACY COUNTY

Chile Vieja

La Sal Vieja

Paso Real

Tenerias

Willamar

ZAPATA COUNTY

Benavides

Davis, South

Jennings/Jennings, West

Lopeno

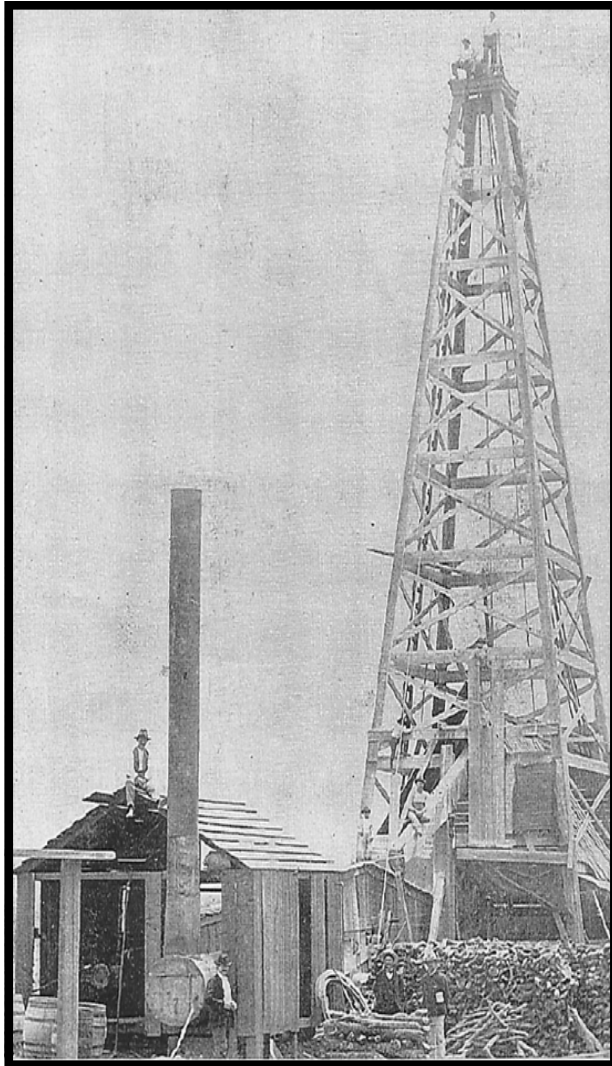
M&F

Pok-A-Dot

ZAVALA COUNTY

El Bano

Call Coastal Bend Geological Library, Maxine: 361-883-2736
1 log -- \$10 each, 5-10 logs \$9 each and 10 + logs \$8.00 each – plus postage



Corpus Christi Geological Society
C/O Javelina Press
P. O. Box 60181
Corpus Christi, TX 78466

Order Form

Mail order form for Wooden rigs-Iron Men. The price is \$75 per copy, which includes sales tax, handling, and postage

Name _____

Address _____

City, State, Zip _____

No. of books _____ Amount enclosed _____

Send to Corpus Christi Geological Society Book Orders

P. O. Box 60181

Corpus Christi, TX. 78466 Tax exempt# if applicable _____

Wooden Rigs—Iron Men

The Story of Oil & Gas in South
Texas

By Bill & Marjorie K. Walraven

Published by the
Corpus Christi Geological Society

OIL MEN
TALES FROM THE SOUTH TEXAS OIL PATCH
DVD
MEMBER PRICE \$25
NON-MEMBER \$30



To Order DVD
Sebastian Wiedmann
swiedmann.geo@gmail.com
If mailed add \$5.00

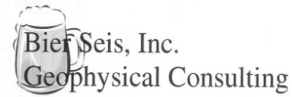


Kyle Barker
Geologist / Geosteering Manager
812.756.2216
kbarker@geotechloggingservices.com

P.O. Box 305 Office: 512.308.8200
Red Rock, TX 78662 Fax: 830.839.4832
www.geotechloggingservices.com

david becker
geologist
o: (361) 884-3613
f: (888) 869-2011
600 leopard st. ste 706
corpus christi, tx 78473
dkbecker1137@sbcglobal.net

David Becker
exploration
geologist



David Biersner, President
19446 Arrowood Place
Garden Ridge, Tx 78266
Cell: 281.744.7457
E-Mail: bierseis@yahoo.com

Field Quality Control
Program Management
Permit Management
Seismic Line Clearing
Supervision



Dawn S. Bissell
Geoscientist

Advent Geoscience Consulting, LLC

Phone: 361-960-2151 253 Circle Drive
Fax: 961-854-2604 Corpus Christi, TX 78411
Email: bisseth@swbell.net Home: 361-854-2635



James Bloomquist
Business Development Manager
jbloomquist@integrityseismic.com

Office 713-357-4706 ext7008 16420 Park Ten Place
Cell 281-660-9695 Suite 240
Fax 713-357-4709 Houston, TX 77084



Elizabeth Chapman
Business development/marketing

11777 Katy Freeway, Ste 570 Houston, TX 77079
office: 281.977.7432 ext 109 fax: 281.829.1788
cell: 713.817.4232 email: elizabeth@flamingoseismic.com

www.flamingoseismic.com



TRAVIS CLARK
GEOLOGIST

DYNAMIC PRODUCTION, INC.

5070 MARK IV PARKWAY
FORT WORTH, TEXAS 76106
PHONE 817.838.1810
FAX 817.838.1824
EMAIL travis.clark@dynprod.net

James L. Claughton
CONSULTING GEOLOGIST

Office | 361-887-2991
Fax | 361-883-4790
Cell | 361-960-2014
clausoie@sbcglobal.net

615 North Upper Broadway
Suite 1935
Corpus Christi, Texas
78401-0779

TEXAS LONE STAR OIL Exploration
PETROLEUM CORPORATION GAS & Production

JEFF COBBS
President - Geologist

615 Leopard St., Suite 336 Office (361) 883-2911
Corpus Christi, Texas 78401-0610
jc@tlspc.com Cell (361) 960-0530

Jim Collins
Geoscientist



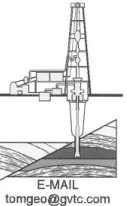
361.537.4034
jim@gulfcoastgas.com



Frank G. Cornish
Consulting Geologist
615 N. Upper Broadway, Suite 1770
Corpus Christi, TX 78401
frank.cornish@gmail.com

361-693-0923 (o)
1-800-510-6810 (f)
361-563-9184 (m)

TOM DAVIDSON
GEOLOGIST



28550 IH-10 WEST SUITE #4
BOERNE, TEXAS 78006

BUS: (210) 844-8963
RES: (830) 981-5883
FAX: (830) 981-5567
CEL: (210) 844-8963

E-MAIL
tomgeo@gvtc.com



Sara Davis
Director of Marketing & Business Development

4805 Westway Park Blvd., Houston, TX 77041
p: 832.554.4301 d: 832.554.4314 c: 713.256.8737
sdavis@seimaxtech.com



FROST BANK PLAZA
802 N. CARANCAHUA, SUITE 1000
CORPUS CHRISTI, TEXAS 78470

LEIGHTON L. DEVINE
EXPLORATION GEOLOGIST

OFFICE: (361) 884-8824
FAX: (361) 884-9623
MOBILE: (361) 510-8872
ldevine@suemaur.com

ONE APEX ENERGY, INC.

CHRISTIAN DOHSE
Consulting Geologist



(361) 877-3431
CHRISTIANDOHSE@GMAIL.COM
CORPUS CHRISTI, TX

Tommy Dubois
Geologist

2627 CR 312
Yoakum, Texas 77995

361-215-0223 tvdubois@yahoo.com



MATTHEW FRANEY
Geologist

VENTEX
Oil & Gas, Inc.

600 Leopard
Suite 904
Corpus Christi, TX 78401

Email: mfraney57@att.net Phone (361) 888-6327

Enrique (Rick) Garza
Operation Supervisor
US Land



Geoscience
Solutions

Rick.Garza@GlobalGeophysical.com
DIRECT +1 713-808-7428
MOBILE +1 361-701-6480
FAX +1 713-808-7528
13927 South Cassman Road
Missouri City, Texas 77489 USA
www.GlobalGeophysical.com

GISLER BROTHERS LOGGING CO., INC.

P.O. BOX 485
106 E. MAIN

RUNGE, TX 78151



Wes Gisler
Bus: (830) 239-4651
Mobile (361) 676-1369

wes@gislerbrotherslogging.com



RAY GOVETT, Ph. D.
CONSULTING GEOLOGIST
361-855-0134

Robert Graham
President
grexploration@gmail.com

Phone 361-882-7681
Fax 361-882-7685
Cell 361-774-3635

GrX Inc.

Exploratory Prospects & Production Development

Mail:
P. O. Box 1843
Corpus Christi, Texas
78403-1843

Office:
606 N. Carancahua, Ste. 610
Corpus Christi, Texas
78401-0634



HART EXPLORATION, LLC.

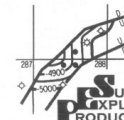
RICK HART
Geologist / Owner

P.O. Box 729
Coldspring, Texas 77331
Cell: 512-626-3053
Email: hartexploration@aol.com

RIVIERA EXPLORATION, LLC

H. TONY HAUGLUM
President

600 LEOPARD ST.
SUITE 1704
CORPUS CHRISTI
TEXAS 78401
PHONE 361.884.1811
FAX 361.884.8071
E-MAIL THAUGLUM@SWBELL.NET



BRENT F. HOPKINS
PRESIDENT AND CEO
GEOLOGIST

FROST BANK PLAZA
802 N. CARANCAHUA, SUITE 1000
CORPUS CHRISTI, TEXAS 78401-0015

OFFICE: (361) 884-8824
FAX: (361) 884-9923
RES: (361) 643-8373
CELL: (361) 215-4855
E-mail: brenth@suemaur.com

James R. Jones
Geologist

7434 Long S Drive
Corpus Christi, TX 78414
361-779-0537
jrjones5426@aol.com



EOG Resources, Inc.
539 N. Carancahua
Suite 900
Corpus Christi, TX 78401-0908
Direct: (361) 887-2691

Randy Lambert
Geological Advisor

Fax: (361) 844-1548
randy_lambert@eogresources.com



Louis R. Lambiotte
Geologist

LMP Petroleum, Inc.
615 N. Upper Broadway, Suite 1770
Corpus Christi, TX 78477
Tel: (361) 883-0923
Fax: (361) 883-7102
E-mail: geology@LMPexploration.com



PATRICK J. McCULLOUGH [President]
patrickm@emeraldbayexp.com

311 Saratoga Boulevard Corpus Christi, Texas 78417
361.852.6195 [e] 361.852.6676 [f] 361.876.7881 [c]

YOUR CARD COULD BE HERE!!!
\$30 FOR 10 ISSUES
AD PRICES PRO-RATED
EMAIL ROBBY AT
ROBERT.STERETT@GMAIL.COM

CURTIS R. MAYO
GEOLOGICAL CONSULTANT

Reserve Analysis Prospect Evaluation
Expert Witness Prospect Generation

Fredericksburg, Texas 78624
Office: 830.992.2938 Cell: 830.765.0628 E-Mail: cmayo@cresec.net



Armando Medina
Owner / Geologist

8610 N. New Braunfels #703 • San Antonio, TX 78217
(210) 538-2170 • amedina@valorexploration.com



J. Mark Miller
President

Phone (361) 883-7700
Fax (361) 883-7701
mark@millersmithgas.com
545 N. Upper Broadway
Suite 400
Corpus Christi, Texas 78476

Wellhead Gas Marketing



Dennis Moore
Formation Evaluation
Wireline - Southern GeoMarket

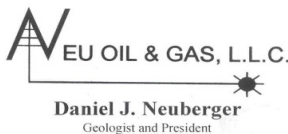
9333 HWY 44
Corpus Christi, TX 78406
Direct: 361-692-3640
Fax: 361-692-3553
Mobile: 361-816-5144
Email: dennis.moore@bakerhughes.com

www.bakerhughes.com

Mailing Address
615 Leopard, Ste. 640
Corpus Christi, Texas 78401-0641
361.882.7888 phone
361.882.7889 fax
361.946.2581 mobile
Contact Address
1701 Southwest Parkway, Ste. 109
College Station, Texas 77840
866.946.2581 phone
866.946.2580 fax
pmueller@melexp.com
www.melexp.com



J. Paul Mueller, Jr.
President



Daniel J. Neuberger
Geologist and President

Austin Office:
712 Winsome Trail
West Lake Hills, Texas 78746

Office (361) 548-7723
Home (512) 306-1223
dan@neuoilandgas.com

Patrick Nye
President
patrick@nyexp.us

Office: (361) 452-1435
Cell: (361) 658-1089
Res: (361) 238-2146



802 N. Carancahua, Suite 1840
Frost Bank Plaza
Corpus Christi, TX 78401
www.nyexp.us



BRIAN E. O'BRIEN

510 Bering Drive
Suite 600
Houston, Texas 77057

Main: 713-783-4883
Fax: 713-783-3039
Res: 713-784-7911
Cell: 713-899-5164
E-mail: bobrien@saxetpetroleum.com



Ken Orlaska
Account Manager

281-497-8440
Direct: 281-249-5051
Fax: 281-558-8096
Cell: 832-455-1818
e-mail: korlaska@geotrace.com
12141 Wickchester Lane, Suite 200
Houston, Texas 77079
www.geotrace.com



**Herradura
Petroleum, Inc.**
JEFF OSBORN
Geologist

711 N. Carancahua, Ste. 1750
Corpus Christi, Texas 78475
e-mail: jef@herradurapetroleum.com

Office: 361-884-6886
Fax: 361-884-9102
Cell: 361-537-2349

Richard M. Parker
Consulting Geologist

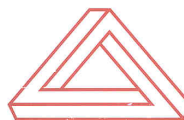
Registered State of Texas Board of Professional Geoscientists
License # 6056

12802 Max Rd.
Brookside Village, Texas 77581
Email: rparker@sbcglobal.net

713-724-4380 Cell 1
713-206-3158 Cell 2
281-412-0745 Home

Lae Prejean
Business Development Manager

800.256.1147
225.247.9038
www.stratagraph.com
lprejean@stratagraph.com



P.O. Box 53848
Lafayette, LA 70505

STRATAGRAPH
Accurate Data. Reliable Solutions.



Beth Priday
Senior Geologist

VirTex Operating Co., Inc.
615 North Upper Broadway
Suite 525, WF168
Corpus Christi, Texas 78477
Bus (361) 882-3046
Fax (361) 882-7427

Mobile: (361)443-5593 • E-mail: bpriday@virtexoperating.com

Minerals Exploration and Mining
Uranium In Situ Leach

Richard M. Rathbun, Jr.
Certified Professional Geologist 9544 / AIPG
Texas Board of Prof. Geoscientists / Lic. No. 4679

921 Barracuda Pl.
Corpus Christi, Texas 78411

(361) 903-8207
rathbunassoc@msn.com



Barry J. Rava
President

Mobile: 281-235-7507
Office: 713-621-7282

barry@icarusog.com
www.icarusog.com

P.O. Box 820253
Houston, TX 77282-0253

Deliveries
1710 S. Dairy Ashford Rd., Ste. 202
Houston, TX 77077



Wireline Services

Weatherford International Ltd.
401 E. Sonterra Blvd., Suite 1
San Antonio, Texas 78258
USA

Sam Roach
US Gulf Coast Wireline Sales

+1 210 930 7568 Direct
+1 210 930 7610 Fax
+1 210 241 2463 Mobile

sam.roach@weatherford.com
www.weatherford.com

First Rock, Inc.

RGR Production First Rock I, LLC

Gregg Robertson

Main Office:
600 Leopard, Suite 1800
Corpus Christi, TX 78401
361-884-0791

San Antonio:
7979 Broadway, Ste 207
San Antonio, TX 78209
210-822-2551

361-884-0863 Facsimile
361-993-6357 Home
361-215-5559 Cell
210-260-0300 Mobile

firstrockinc@msn.com



Alvin Rowbatham
Sales, Gulf of Mexico

Main +1 713 789 7250
Direct +1 281 781 1065
Fax +1 713 789 7201
Mobile +1 832 372 2366
alvin.rowbatham@iongeo.com

2105 CityWest Blvd. | Suite 900
Houston, TX 77042-2839 USA

TOM SELMAN
selmanlog.com
tselman@selmanlog.com

Ofc. (432) 563-0084
(800) 578-1006
Cell (432) 288-2259



GEOLOGICAL CONSULTING / SURFACE LOGGING SERVICES

P.O. Box 61150 Midland, TX 79711 4833 Saratoga #624 Corpus Christi, TX 78413 P.O. Box 2993 Rock Springs, WY 82902



Petrophysics, Inc.
Velocity Surveys • Synthetics • Sonic Log Data

Joe H. Smith
President

P.O. Box 863323
Plano, Texas 75086

713.560.9733
jsmith@petrophysics.com
www.petrophysics.com

Crossroads Exploration

Gloria D. Sprague
Geologist

Timpon Building 189 N. First Street, Suite 111
Timpon, Texas 75975
E-Mail: gsprague@usawide.net
Office: (936) 254-3600
Fax: (936) 254-3602
Mobile: (936) 488-9428

Charles A. Sternbach, Ph.D
President

Star Creek Energy Company
Oil and Gas Exploration

800 Wilcrest Drive, Suite 230
Houston, Texas 77042
office: 281.679.7333
cell: 632.567.7333
carbodude@gmail.com



www.starcreekenergy.com

YOUR CARD COULD BE HERE!!!
\$30 FOR 10 ISSUES
AD PRICES PRO-RATED
EMAIL ROBBY AT
ROBERT.STERETT@GMAIL.COM

THOMAS W. SWINBANK

CERTIFIED PETROLEUM GEOLOGIST
PRESIDENT

STRIKE OIL & MINERALS CORP.
P.O. Box 1399
GEORGETOWN, TEXAS 78627
PHONE/FAX 512-863-7519
HOME 512-863-7803
CELL 512-876-9565

Dennis A. Taylor
President and Chief Geologist
dennis@amshore.com

Off: (361) 888-4496
Fax: (361) 888-4558
Direct Line: (361) 844-6728
Cell: (972) 672-9916



AMERICAN SHORELINE, INC.

AMSHORE US WIND, LLC
802 N. Carancahua Street, Suite 1350
Corpus Christi, Texas 78401-0019
www.amshore.com

Environmental

Exploration & Production

JEANIE TIMMERMANN
GEOSCIENTIST
TX LICENSE #2289

7214 Everhart #9
Corpus Christi, TX 78413

(361) 991-7451
jimmerrmann74@msn.com



Jim Trevillo
Senior Geoscientist

1330 Post Oak Boulevard
Suite 600
Houston, Texas 77056

Direct: 713.438.6773
Main: 713.826.7765
Fax: 713.826.7775
Cell: 713.826.9392

jtrevillo@davcos.com

www.davispetroleumcorp.com



10001 Richmond Avenue
Houston, TX 77042-4299
P.O. Box 2469 (77252-2469)
Tel: 713-689-6662
Fax: 713-689-1089
Mobile: 281-615-6827
C.Tutt@slb.com

Chris O. Tutt
Sales Representative
NAM Sales



WILLIAM A. WALKER, JR.
Certified Petroleum Geologist
bwalker@stalkerenergy.com

1717 West 6th Street, Ste. 230 • AUSTIN, TX 78703
2001 Kirby Dr., Ste. 950 • HOUSTON, TX 77019

AUSTIN
512.457.8711
cell: 512.217.5192
fax: 512.457.8717
HOUSTON
713.522.2733
cell: 512.217.5192
fax: 713.522.2879

SEBASTIAN P. WIEDMANN
GEOSCIENTIST

WILSON PLAZA WEST
505 N. CARANCAHUA, SUITE 500
CORPUS CHRISTI, TEXAS 78401
MOBILE (361) 946-4430
swiedmann.geo@gmail.com



Dave Willis
Onshore Sales

Main +1 713 789 7250
Direct +1 281 781 1035
Mobile +1 281 543 6189
Fax +1 713 789 7201
dave.willis@iongeo.com

2105 CityWest Blvd. | Suite 900
Houston, TX 77042-2839 USA



10001 Richmond Avenue
Houston, Texas 77042-4299
P.O. Box 2469 (77252-2469)
Tel: 713-689-2757
Fax: 713-689-1089
Mobile: 281-658-5263
CYanez@slb.com

Charles Yanez
Manager
Shared Value Optimization